

## Prolonged Record of Hydroclimatic Changes at Antoniadi Crater, Mars



### Key Points:

- Antoniadi crater is the site of an ancient lake that was punctuated by locally and regionally wet conditions between 3.7 and 2.4 Ga
- Antoniadi crater likely records at least four episodes of surface runoff
- The river and lake systems at Antoniadi were probably active for  $10^3$ – $10^6$  years, supporting long-lived fluvial activity under arid climates

### Supporting Information:

Supporting Information may be found in the online version of this article.

### Correspondence to:

A. S. Zaki,  
[azaki@caltech.edu](mailto:azaki@caltech.edu)

### Citation:

Zaki, A. S., Edgett, K. S., Pajola, M., Kite, E., Davis, J. M., Mangold, N., et al. (2023). Prolonged record of hydroclimatic changes at Antoniadi crater, Mars. *Journal of Geophysical Research: Planets*, 128, e2022JE007606. <https://doi.org/10.1029/2022JE007606>

Received 4 OCT 2022  
 Accepted 15 JUN 2023














### Author Contributions:

**Conceptualization:** A. S. Zaki, K. S. Edgett, M. Pajola, E. Kite, N. Mangold, A. S. Madof, S. Gupta, S. Castellort  
**Data curation:** N. Thomas, G. Cremonese

**Formal analysis:** A. S. Zaki, K. S. Edgett, M. Pajola, E. Kite, J. M. Davis, N. Mangold, A. Lucchetti, P. Grindrod, C. M. Hughes, S. Castellort

**Funding acquisition:** A. S. Zaki, S. Castellort

**Investigation:** A. S. Zaki, E. Kite, J. M. Davis, N. Mangold, A. Lucchetti, M. Schuster, S. Gupta, S. Castellort

A. S. Zaki<sup>1,2</sup> , K. S. Edgett<sup>3</sup> , M. Pajola<sup>4</sup> , E. Kite<sup>5</sup> , J. M. Davis<sup>6</sup> , N. Mangold<sup>7</sup> ,  
 A. S. Madof<sup>8</sup> , A. Lucchetti<sup>4</sup> , P. Grindrod<sup>9</sup> , C. M. Hughes<sup>10</sup> , K. Sangwan<sup>11</sup> , N. Thomas<sup>12</sup>,  
 M. Schuster<sup>13</sup> , S. Gupta<sup>11</sup>, G. Cremonese<sup>4</sup> , and S. Castellort<sup>1</sup>

<sup>1</sup>Department of Earth Sciences, University of Geneva, Geneva, Switzerland, <sup>2</sup>Now at Division of Geological and Planetary Sciences, California Institute of Technology, Pasadena, CA, USA, <sup>3</sup>Malin Space Science Systems, Inc., San Diego, CA, USA, <sup>4</sup>INAF-Osservatorio Astronomico di Padova, Padova, Italy, <sup>5</sup>Department of the Geophysical Sciences, University of Chicago, Chicago, IL, USA, <sup>6</sup>Department of Earth and Planetary Sciences, Birkbeck, University of London, London, UK, <sup>7</sup>Laboratoire de Planétologie et Géosciences, UMR6112 CNRS, Nantes Université, Université d'Angers, Le Mans Université, Nantes, France, <sup>8</sup>Chevron, Global Exploration, Houston, TX, USA, <sup>9</sup>Department of Earth Sciences, Natural History Museum, London, UK, <sup>10</sup>Department of Geosciences, University of Arkansas, Fayetteville, AR, USA, <sup>11</sup>Department of Earth Sciences and Engineering, Imperial College London, London, UK, <sup>12</sup>Space Research and Planetology Division, University of Bern, Bern, Switzerland, <sup>13</sup>UMR 7063, CNRS, Institut Terre et Environnement de Strasbourg, Université de Strasbourg, Strasbourg, France

**Abstract** The first billion years of Martian geologic history consisted of surface environments and landscapes dramatically different from those seen today, with flowing liquid water sculpting river channels and ponding to form bodies of water. However, the hydro-climatic context, the frequency, and the duration under which these systems existed remain uncertain. Addressing these fundamental questions may improve our understanding of early Mars climate. Here, we reconstruct a long-lived archive consisting of an array of fluvial systems inside the Antoniadi crater—one of the largest lake basins on Mars ( $9.58 \times 10^4$  km<sup>2</sup>). We found that the fluvial activity occurred throughout four major intermittent active intervals during the Late Noachian to Early Amazonian (~3.7 to >2.4 Ga). This resulted in at least two major lakes, which formed during periods of markedly increased surface runoff production. The record of these four riverine phases is preserved in fluvial ridges, valley networks, back-stepping or down-stepping fan-shaped landforms, and terrace-like formations within an outlet canyon. These morphologies point to lake-controlled base-level fluctuations suggestive of episodic precipitation-fed surface runoff punctuated by intermittent catastrophic floods that were capable of breaching crater-lake rims and incising outlet canyons. Fluvial-deposit thickness, junction angles of channels, and lake morphometry suggest that riverine systems lasted at least  $10^3$ – $10^6$  years and episodically occurred under primarily arid and semi-arid climates. These findings place new regional constraints on the fluvial frequency, longevity, and climatic regime of one of the largest Martian lakes, thereby bolstering the hypothesis that episodic warming likely punctuated the planet's early history.

**Plain Language Summary** The planet Mars is now a vast desert. However, geologic evidence points to radically different kinds of landscapes in the past, with precipitation-fed ancient rivers and lakes. As a consequence, questions have been raised about the climatic and environmental contexts that persisted during the formation of these hydrological records. Here, we have used high-resolution remotely sensed data to constrain the volumes, frequency, and periodicity of an array of water-formed landforms inside one of the largest lake systems on Mars that occupy the Antoniadi crater. We demonstrate that the Antoniadi crater was intermittently wet, hosting multiple rivers and at least two main bodies of standing water between 3.7 and 2.4 Ga. The morphometries of the lake and river systems imply that they episodically survived between a few thousand and 1 million years under arid climates. These findings make Antoniadi an interesting site for future Mars exploration dedicated to the potential ancient habitability of Mars because of such long-lived fluvial history.

© 2023. The Authors.

This is an open access article under the terms of the [Creative Commons Attribution License](https://creativecommons.org/licenses/by/4.0/), which permits use, distribution and reproduction in any medium, provided the original work is properly cited.

## 1. Introduction

Multiple geologic and geochemical proxies collected over the past decades suggest that wetter environments prevailed in the early Martian climate, primarily during the Noachian and the Hesperian (~3.9–3.5 Ga). This view is strongly supported by imprints of ancient valley networks, depositional rivers, lakes, and fan-shaped deposits that might have existed in arid to semiarid environments (e.g., Bahia et al., 2022; Davis et al., 2016; Dickson

**Methodology:** A. S. Zaki, M. Pajola, E. Kite, J. M. Davis, N. Mangold, P. Grindrod, C. M. Hughes, N. Thomas, M. Schuster, S. Castellort  
**Supervision:** K. S. Edgett, N. Mangold, S. Castellort  
**Visualization:** A. S. Zaki, A. S. Madof  
**Writing – original draft:** A. S. Zaki, K. S. Edgett, M. Pajola, E. Kite, J. M. Davis, N. Mangold, A. S. Madof, C. M. Hughes, M. Schuster, S. Castellort  
**Writing – review & editing:** A. S. Zaki, K. S. Edgett, M. Pajola, E. Kite, J. M. Davis, N. Mangold, A. S. Madof, A. Lucchetti, P. Grindrod, C. M. Hughes, N. Thomas, M. Schuster, S. Castellort

et al., 2020; Grotzinger et al., 2015; Goudge et al., 2021; Hynes et al., 2010; Kite, 2019; Kite et al., 2019; Malin & Edgett, 2000, 2003; Mangold et al., 2021a; Stack et al., 2020; Williams et al., 2013; Wilson et al., 2021). Most of these water-formed landforms were likely formed in response to surface runoff, with groundwater sapping playing a lesser role (Higgins, 1982; Howard et al., 2005; Irwin et al., 2005; Lamb et al., 2006; Salese et al., 2019; Seybold et al., 2018). However, theoretical models have raised serious questions about the frequency, volume, and duration of the water that flowed on the early Martian surface, highlighting the difficulty of sustaining temperatures greater than the freezing point of water (e.g., Wordsworth et al., 2013, 2015). Such temperatures are not consistent with the hypothesis of a volume of liquid water that is sufficiently large enough to form a set of large, planetwide perennial lakes as well as carve extensive valley networks unless these deposits formed episodically during transient warm and wet intervals (El Maarry et al., 2010; Fassett and Head, 2008a, 2008b; Grotzinger et al., 2015; Hynes et al., 2010; Kite et al., 2021; Wordsworth et al., 2013, 2021). To tackle this fundamental issue, it is necessary to use robust geological clues that provide critical information that climate modelers can use as benchmarks for simulating Mars' past environments. Among Mars' geomorphological features, dry, eroded remnants of fluvial systems and ancient lake basins are abundant, globally distributed (e.g., Cardenas et al., 2017; Davis et al., 2016; Dickson et al., 2020; Fassett & Head, 2008a, 2008b; Goudge et al., 2021; Hynes et al., 2010), and serve as rich repositories for investigating past Martian environments (e.g., Grotzinger et al., 2015; Mangold et al., 2021a; Williams et al., 2013); they are also considered essential targets for investigating potential habitability on early Mars (e.g., Grotzinger et al., 2015).

An extensive catalog of 265 crater lake candidates, based on outlet canyons and fans, has been created from several studies (e.g., Cabrol & Grin, 1999; Fassett & Head, 2008a, 2008b; Goudge et al., 2015, 2016; Irwin et al., 2005; Stucky de Quay et al., 2020). These candidate lakes can provide critical information as they represent a condensed archive of climatically driven fluvial processes that may have affected paleo-watersheds. We, therefore, reconstructed the systems that shaped the fluvial history of one of the largest open-basin lakes on Mars, Antoniadi crater. This impact basin has a diameter of ~410 km, is located at 60.94°E, 21.10°N to the northwest edge of Syrtis Major Planum, and was likely formed nearly 4 Ga (Figure 1) (e.g., De Blasio, 2022; Fassett & Head, 2008a, 2008b). The flat part of the crater interior was interpreted by Tanaka (2014) to have been resurfaced by volcanic materials during the Early Hesperian. Additionally, previous work has proposed that during its early history,  $5.5 \times 10^5$  km<sup>2</sup> of drainage basin supplied the Antoniadi crater with  $3.10 \times 10^4$  km<sup>3</sup> of water, forming a large body of standing water that was responsible for creating an outlet canyon (Fassett and Head, 2008a, 2008b), ~3.8 Ga (De Blasio, 2022).

Prior work at Antoniadi crater has primarily concentrated on mapping the extent of large bodies of water in the region (Fassett and Head, 2008a, 2008b; Goudge et al., 2015), mapping the branched rivers standing as ridges in the modern landscape in the middle of the crater (Davis et al., 2016), or interpreting those branched ridges (e.g., De Blasio, 2022; Mangold et al., 2021b). The aforementioned research found that there is evidence of two large bodies of water, inverted channels, and possible involvement of volcanic or biogenic processes in the formation of the branching ridges (e.g., Davis et al., 2016; De Blasio, 2022; Fassett & Head, 2008a, 2008b; Goudge et al., 2015; Mangold et al., 2021b). This diverse array of water-formed landscapes provides a spectacular window into early Mars's environmental and climatic history.

In this paper, we constrain the frequency, duration, and climatic regime of fluvial activity during the formation and the evolution of the Antoniadi crater by reconstructing the paleo-morphology of various fluvial systems that fed this water body. Attaining this objective necessitates mapping and measuring the morphologies of the preserved remnants of ancient fluvial systems in and around Antoniadi, describing the depositional morphology and stratigraphy of the basin's fluvial sedimentary deposits, estimating the fluvial discharge and precipitation, constraining the aridity, and modeling age relationships. This study provides new regional constraints on the river and lake-forming environments that existed in and around the Antoniadi crater on early Mars.

## 2. Materials and Methods

### 2.1. Characterizing the Morphology and Stratigraphy of the Fluvial Systems

To explore the morphology and sedimentology of ancient fluvial deposits within Antoniadi crater and its proposed outlet canyon, as well as an attempt to extrapolate the depositional environments contained within, our study used images from the Mars Reconnaissance Orbiter (MRO) Context Camera (CTX; ~6 m/pixel; Malin

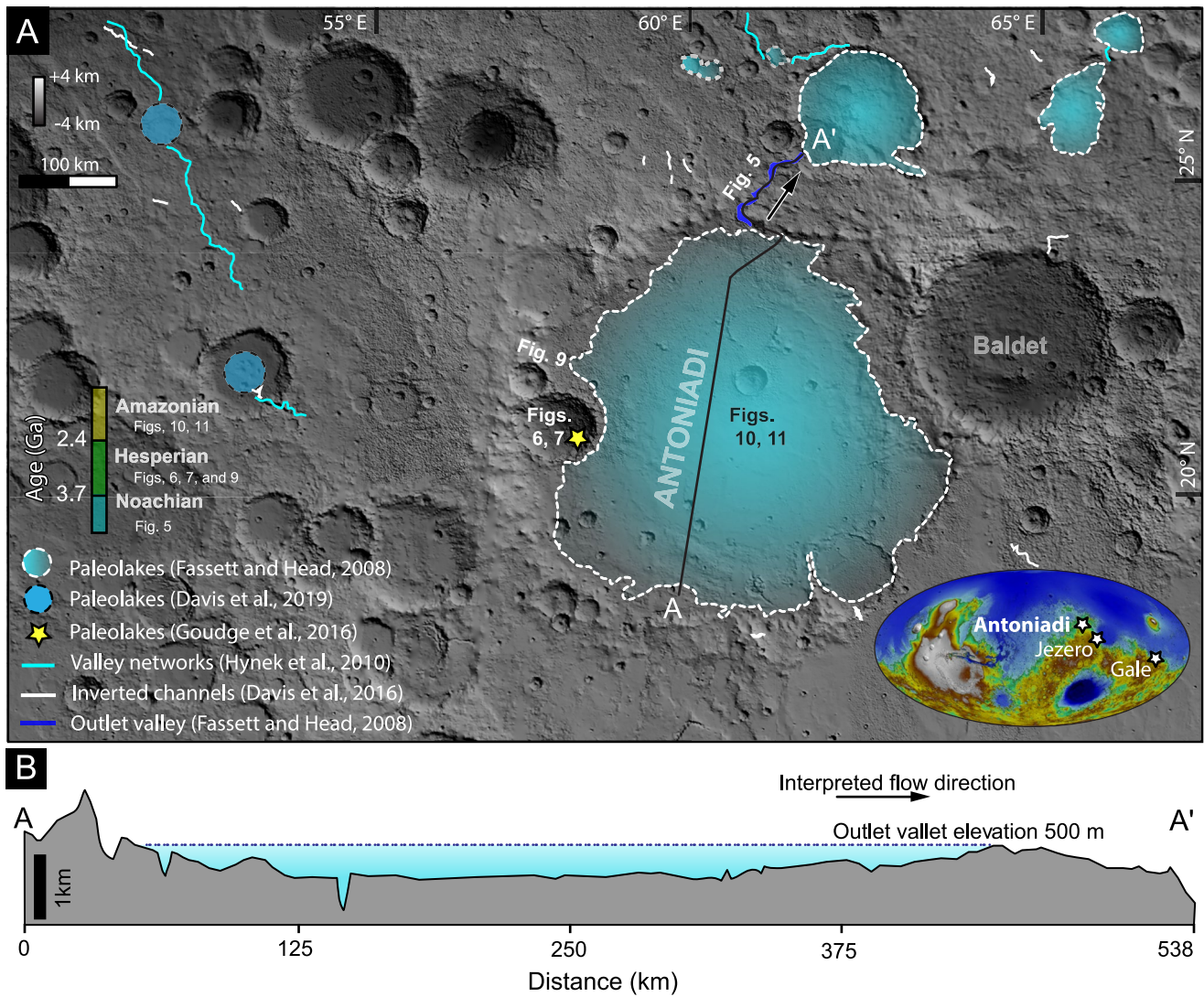


**Figure 1.** Antoniadi crater paleolake basin, located at  $\sim 60.94^{\circ}\text{E}$ ,  $21.10^{\circ}\text{N}$  (Fassett and Head, 2008a, 2008b). (a) Overview of shaded relief topographic map derived from the blended MOLA/HRSC gridded topographic map (200 m/pixel) showing the inferred paleolake occupying Antoniadi crater based on outlet canyon ( $\sim 500$  m; Fassett & Head, 2008a, 2008b). It also shows the distribution of the other previously proposed water-formed landforms, including valley networks (Hynek et al., 2010), inverted channels (Davis et al., 2016), and other paleolakes (Davis et al., 2019; Fassett and Head, 2008a, 2008b; Goudge et al., 2016). The locations of fluvial systems discussed in this paper and their ages are also shown. The age scale shows where the figures described in the text are. The colors of the age scale represent the different timescales. (b) Profile A-A' along the Antoniadi paleolake shows that the water breached the rims at  $\sim 500$  m, carving an outlet canyon.

et al., 2007), the Colour and Stereo Surface Imaging System (CaSSIS;  $\sim 4.6$  m/pixel; Thomas et al., 2017), and the High-Resolution Imaging Science Experiment (HiRISE;  $\sim 25$  m/pixel; McEwen et al., 2007). In addition to the image data (Table S1 in Supporting Information S1), we used three digital terrain models (DTMs) from HiRISE ( $\sim 1$  m/pixel) and CTX ( $\sim 20$  m/pixel), a pair of stereo images that were specifically constructed for this study using the Integrated Software for Imaging Spectrometers (ISIS), and SocetSet software (following the methodology of Kirk et al., 2008). We also used blended MOLA/HRSC gridded topographic maps (200 m/pixel) for vast areas that lack CTX and HiRISE stereo-pair coverage. Using stratigraphic correlations between the Antoniadi crater's rim and floor and the observed fluvial systems, we were able to divide the mapped fluvial landforms into four stages of deposition based on their relationship to Antonaidi's evolution. Also, morphometric characteristics, such as channel length, pattern, and width, were considered to refine our classification. Our observations and measurements of the fluvial landform morphometrics, including channel width and fluvial ridge thickness, were made using the measure distance and area tool in the ArcMap and Global mapper software packages (Figure 2).



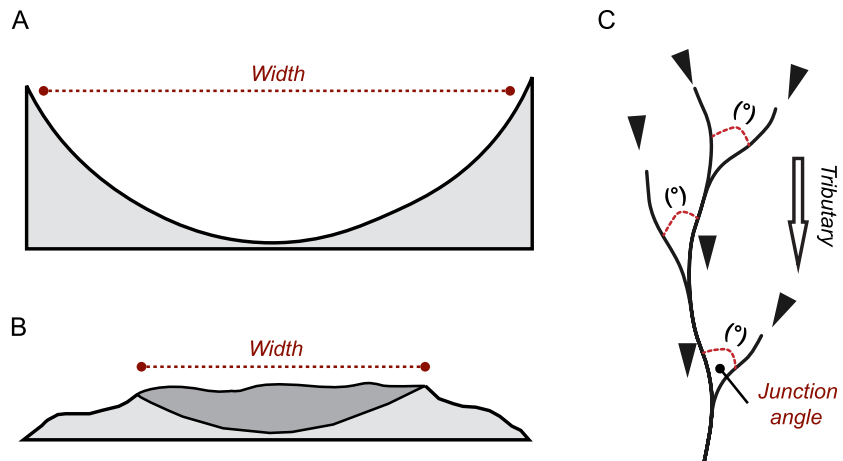


**Figure 2.** Cartoon showing how we measured the channel and ridge width as well as the junction angles.

## 2.2. Chronology—Crater Retention Age and Stratigraphic Relationships

Although the age of the fluvial systems within the Antoniadi crater is unknown, crater counts per unit surface area (of specific geologic materials or geomorphic surfaces) can provide a means to estimate the upper limit of their age (e.g., Hartmann & Neukum, 2001; Michael, 2013); however, these measurements sometimes yield significant uncertainties that may lead to incorrect results (e.g., Warner et al., 2015). To correct these inconsistencies, we calibrated stratigraphic ages from published geological maps (Figure 3; Tanaka, 2014) to estimates obtained from crater counting. Also, we consider the stratigraphic relationships between the different phases of fluvial erosion and deposition (Figures 4–9). We carried out this crater-size frequency analysis using the Craterstats 2 software at three sites (Figures 4–6, 8, and 9; Michael & Neukum, 2010; Neukum, 1983).

## 2.3. Constraining the Paleo-Hydraulics and Climate Regime From Images

Many studies have used channel width as a proxy to estimate flow discharge on Earth and Mars (e.g., Dietrich et al., 2017; Eaton, 2013; Jacobsen & Burr, 2016, 2018; Kite et al., 2019; Williams et al., 2009). However, most of the paleo-river landforms within Antoniadi crater are eroded systems, leaving what used to be the river bed standing as elevated ridges in the present-day landscape (e.g., Zaki et al., 2021). Previous work in terrestrial environments estimated that discharge calculations based on the width of the fluvial ridge are a factor of 1–20 greater than that inferred from slope and grain size information (e.g., Hayden et al., 2019; Hayden, Lamb, & Carney, 2021; Williams et al., 2009; Zaki et al., 2022). Despite the marked uncertainties involved in using these approaches, it is more feasible to quantify flow discharge rates on Mars using the former methodology, primarily because of the difficulty in measuring grain size and channel thickness from the available data (Kite et al., 2019). Also, whatever the uncertainty, the main objective of quantifying the discharge is to assess the magnitude of change between the different episodes. This would help track the development of fluvial history throughout the changing climate. Therefore, we selected the discharge-width relationship described in Eaton (2013), scaled to Martian gravity by Kite et al. (2015), and assumed that rivers on early Mars flowed slower than those on Earth (Equation 1). Here, we measured 94 ridges and channel width from three different fluvial intervals (Table S2 in Supporting Information S1; Figure 2).

$$Q_w = [W / (1.257 \times 3.35)]^{1.8656} \quad (1)$$

We also use valley geometry, particularly angle junction, to determine whether Mars' environment at the time of the incision was dry or humid. Drainage networks in arid zones with higher surface runoff branch at substantially narrower angles ( $41^\circ$ ) than those in humid settings ( $72^\circ$ ) which experience more groundwater flow (e.g., Cang & Luo, 2019; Devauchelle et al., 2012). The branching angles can also be influenced by the slope (Castellort & Yamato, 2013; Castellort et al., 2009); however, Seybold et al. (2018) used a global analysis of junction angles on Mars and some terrestrial analogs on Earth to suggest that gradient variations were unlikely to affect the use of the junction angle as a proxy for climatic regimes. As such, we measured  $\sim 300$  junction angles to determine



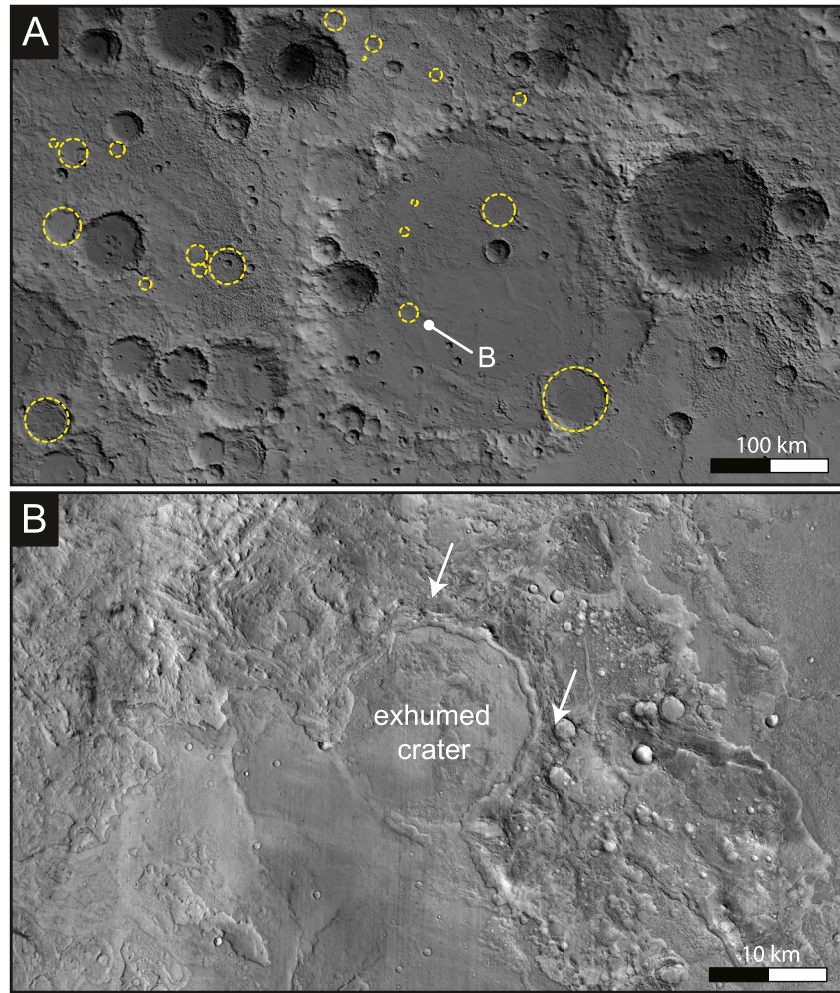


**Figure 3.** (a) Distribution of wholly eroded craters. (b) Context Camera image of a 17-km-diameter exhumed meander, indicating significant erosion rates at Antoniadi crater.

whether these drainage networks formed under relatively arid or humid Martian conditions (Figure 2, Figure S2 and Table S2 in Supporting Information S1).

We also used lake area, lake volume, and watershed area of the Antoniadi crater that were constrained from MOLA and HRSC data by Fassett and Head (2008a, 2008b) to cross-validate the minimum aridity index ( $AI_{\min}$ , Equation 2) and bring a new constraint on the minimum precipitation ( $P_{T,\min}$ , Equation 3). The aridity index ranges from less than 0.05 for hyper-arid to more than  $>0.75$  for hyperhumid environments. This approach has already been used to quantify precipitation and aridity on Mars (Stucky de Quay et al., 2020).

$$AI_{\min} = A_{L,O} / [A_{L,O} + A_{W,O}] \quad (2)$$

$$P_{T,\min} = V_{L,O} / [A_{L,O} + A_{W,O}] \quad (3)$$

where  $A_{L,O}$  is the lake area ( $\text{km}^2$ ),  $A_{W,O}$  represents the watershed area ( $\text{km}^2$ ), and  $V_{L,O}$  is the lake volume ( $\text{km}^3$ ).

#### 2.4. Constraining the Duration of Fluvial Activity

In order to approximate the duration of fluvial activity, we used thickness measurements of fluvial depositional rivers (fluvial ridges) as a proxy. This can be calculated simply by dividing the ridge thicknesses by the

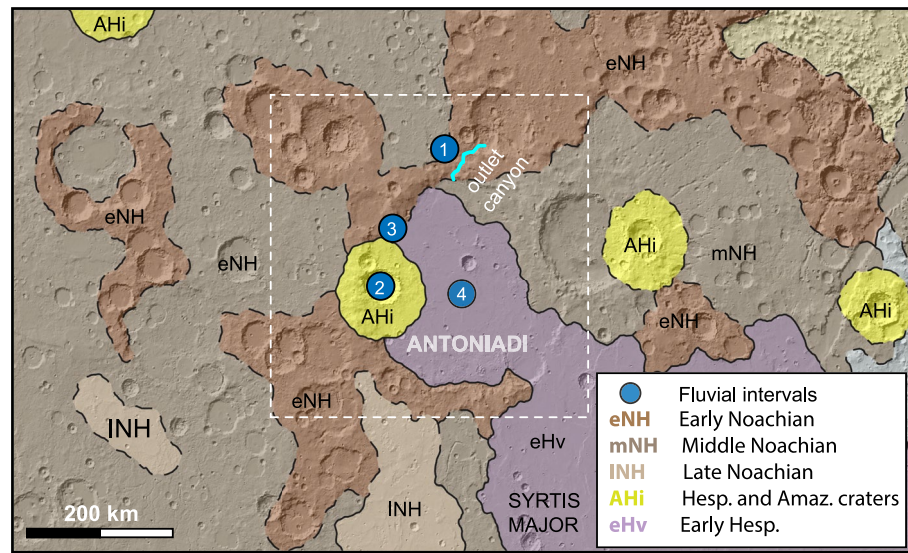


**Figure 4.** A geological map showing the locations of the four fluvial intervals (adapted from Tanaka, 2014). The map indicates that the first interval was carved within the eNH formation (early Noachian), followed by the second interval during AHi (Hesperian to Early Amazonian). The third interval spanned the early Hesperian, after which the crater floor underwent resurfacing due to volcanic activity (eHv). The final interval occurred subsequent to this resurfacing event.

aggradation rates of Earth's fluvial depositional systems. Most of the terrestrial aggradation rates from ancient fluvial systems range from 0.01 to 0.7 m/kyr (Colombera et al., 2015).

### 3. Observations and Results

#### 3.1. Geomorphic and Chronologic Evolution

The Antoniadi crater and its surroundings show dark-toned material resurfacing the floor, coupled with extensive erosional surfaces, including fluvial ridges and exhumed craters, which suggests a substantial exhumation and burial role in shaping its geological history. We discuss the fluvial ridges in detail in the following sections since they represent a significant part of Antoniadi's fluvial history. Here, we show that the erosion is not only at the scale of fluvial ridges (a few to tens of meters of vertical erosion based on the ridge thickness). Instead, our mapping of 18 completely eroded craters with diameters ranging from 1 to 70 km suggests that such craters would have depths of up to a few kilometers (now eroded away, recording a few kilometers of erosion, Figure 4). Despite this significant burial and erosion, a regional-scale survey of the Antoniadi crater's fluvial landforms shows relics of various fluvial erosional and depositional systems, including fluvial ridges, valley networks, fan-shaped deposits, and the outlet canyon, which can be traced to the crater's western and northern rims as well as its center. The patchiness of the fluvial record in the eastern and southern rims is likely attributable to differential erosion or burial by subsequent volcanic episodes; for example, Hesperian lava flows (Figure 4; Tanaka, 2014). The fluvial system morphology is locally sourced and varies significantly. We used morphologic attributes and stratigraphic relationships to classify these features into four key fluvial intervals over nearly 1 billion years (Figure 4).

Our investigation of stratigraphic relationships reveals that the earliest unit dates back to the early and mid-Noachian eras, which apparently once filled the entire basin. Subsequently, the crater was resurfaced by volcanic products from the early Hesperian period. Finally, a Hesperian to Amazonian impact crater is superimposed on the western rim of the Antoniadi, marking the concluding stage of the basin's geologic evolution.

In correlation with our scrutiny of fluvial remnants, we found that the outlet valley was incised into early Noachian rocks (Section 3.1.1), followed by fluvial landforms that are remarkably preserved within the Hesperian-Amazonian crater (Section 3.1.2). The Hesperian-Amazonian crater's ejecta displayed a source-to-sink fluvial system overlaid by volcanic products (Section 3.1.3), which was likely accumulated during the early Hesperian era. Above the volcanic unit, we identified a suite of branched ridges situated in the center of the Antoniadi basin (Section 3.1.4). This feature likely represents the final phase of fluvial activity. Collectively,



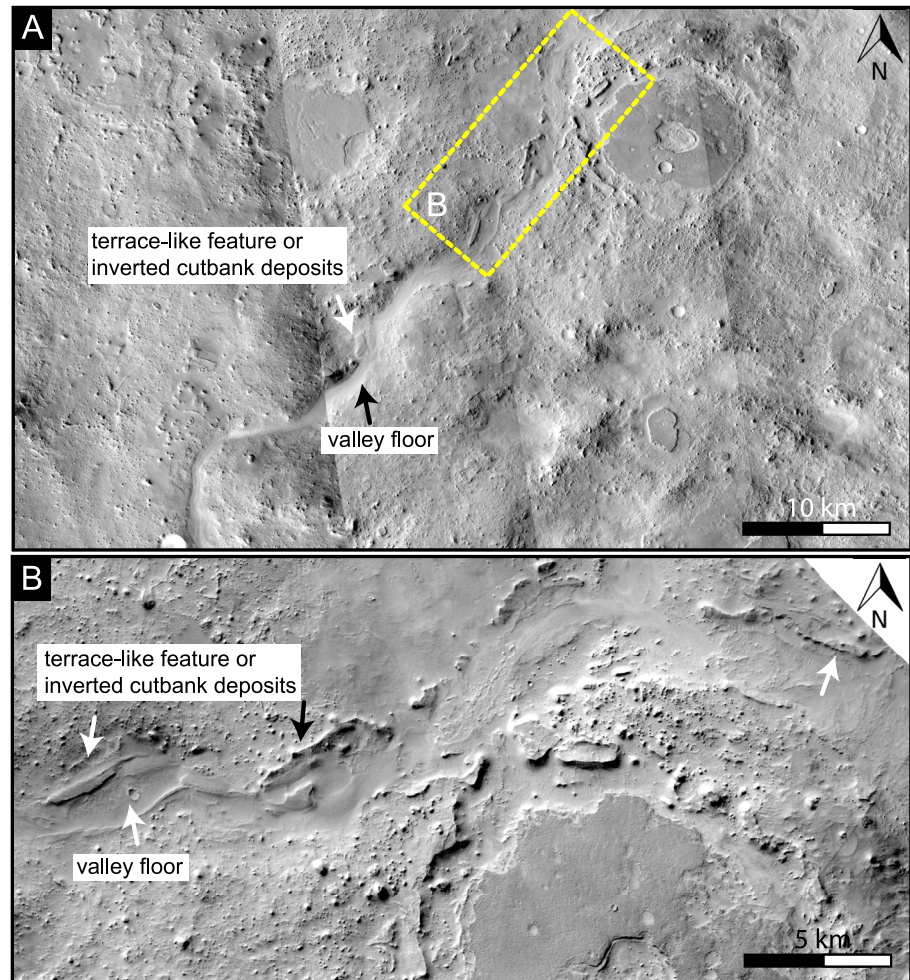


**Figure 5.** (a, b) Mosaic of four Context Camera images of the outlet canyon that formed due to floods breaching the Antoniadi crater rims. We recognize terrace-like features that formed within the outlet canyon, implying that the formation of the outlet canyon and the hydrologic cycle within Antoniadi was episodic (P20\_008967\_2064\_XN\_26N299W; N10\_066223\_2072\_XN\_27N299W; N05\_064482\_2071\_XI\_27N298W; B01\_010101\_2053\_XN\_25N298W).

these observations and their stratigraphic correlations suggest the existence of a record of at least four intervals of fluvial activity, stretching from the early Noachian to beyond the early Hesperian period.

### 3.1.1. The Early Growth of the Antoniadi Paleolake (>3.7 Ga)

We traced the Antoniadi crater rim to map the fluvial systems that were involved in filling the whole Antoniadi crater, forming an ancient lake (Figure 1 and Figure S1 in Supporting Information S1). These systems were estimated to have occurred over an area of 550,000 km<sup>2</sup> (Fassett & Head, 2008a, 2008b); however, we were unable to detect any relics from the first episode of fluvial activity, except an outlet canyon (Figure 5). This prominent erosional feature occurs in the northern rim of Antoniadi crater at an elevation of ~500 m; it is clustered in a ~1–4 km wide, ~300 m depth, and ~100 km long drainage system that is presumed to have directed water and sediments into another crater (Figure 5). The outlet canyon exhibits well-preserved interior terrace-like features or inverted cutbank deposits (Figure 5).

Based on the lake morphometries, including watershed, lake volume, and lake area, Fassett and Head (2008a, 2008b) found that the lake empirically required minimum precipitation of ~56 m to fill the entire lake (PT, min. Equation 3), reach an elevation of ~500 m, and incise an outlet canyon. Using the previous lake parameters in Equation 2, we calculate the minimal aridity index to be 0.148, suggesting an arid environment, given that the



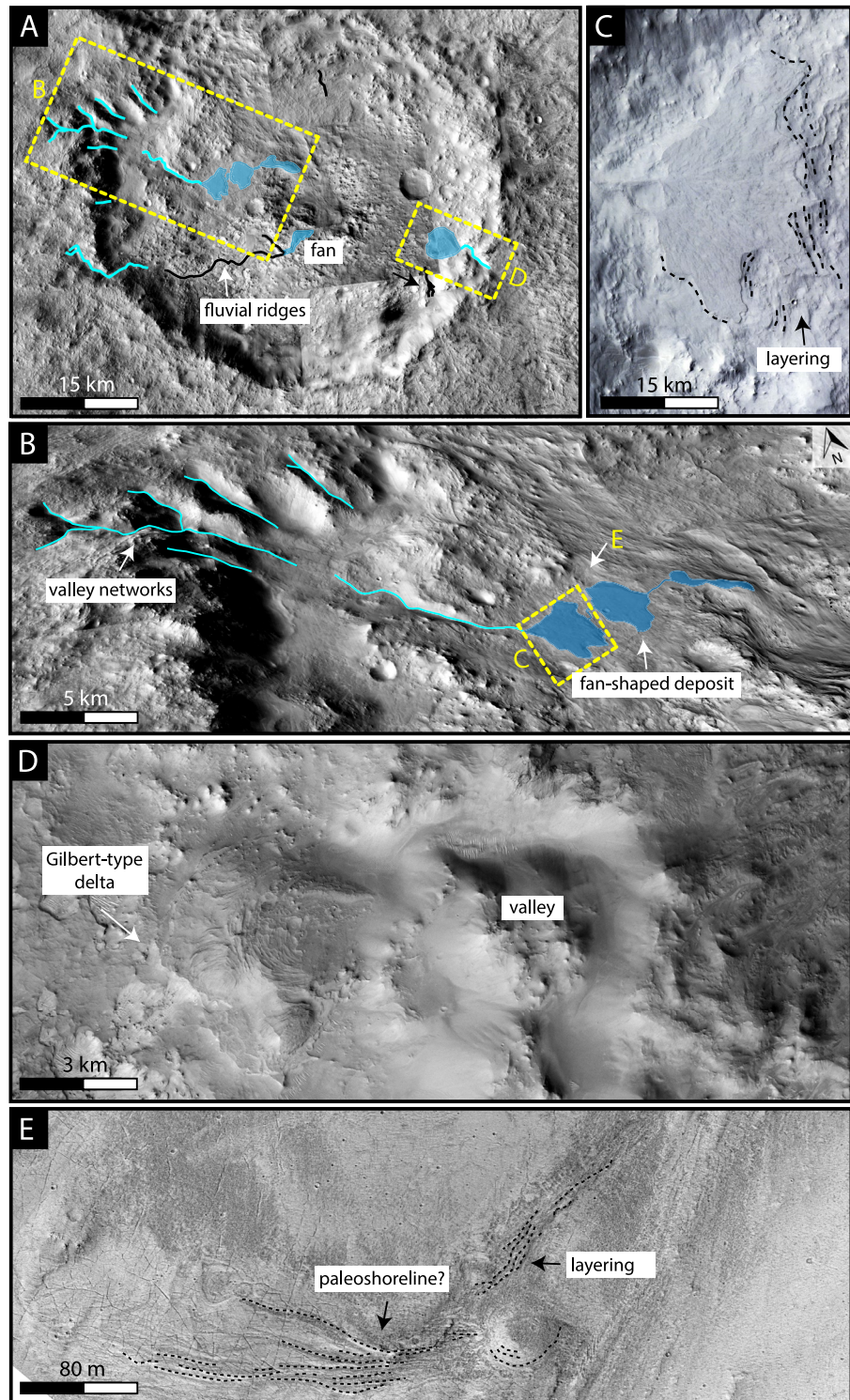


**Figure 6.** (a) Context Camera (CTX) mosaic shows the source-to-sink of three fluvial systems that developed within an unnamed ~65 km diameter (21°28′45.44″N; 57°52′55.65″E). (b) Perspective view from CTX mosaic derived from Google Mars displays one of these fluvial systems that record valley networks carved in a bedrock, transferring sediments and water through a trunk valley and forming multiple fans accumulated at various elevations. (c) Colour and Stereo Surface Imaging System image showing sedimentary structures of one of these fans; multiple layers are stacked within the fan (MY35\_008677\_022\_0). (d) CTX image showing an ideal Gilbert-type delta within the crater (P16\_007161\_2011\_XN\_21N301W). (e) Observed layering within the crater may indicate either a paleoshoreline or crater ejecta (HiRISE: ESP\_066144\_2015).

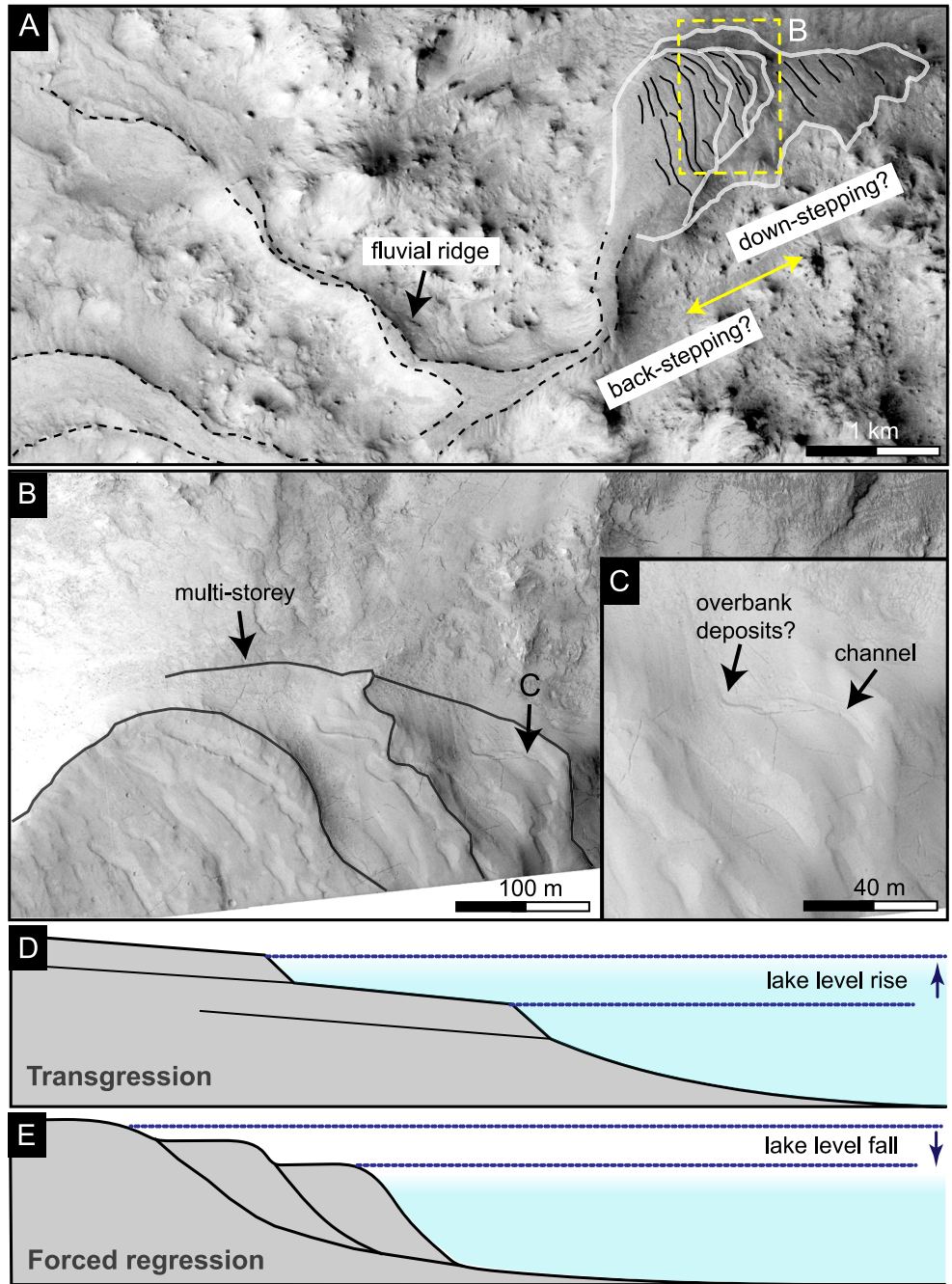


**Figure 7.** (a) Portion of the fluvial system within the same crater shows fluvial ridges connected to multi-storey fan-shaped deposit (CTX: P13\_005948\_2017\_XN\_21N302W). (b, c) High-Resolution Imaging Science Experiment portions show trajectories of either back-stepping or down-stepping of the most bottom part of the delta; the undulating margin of the delta layers might correspond to either erosional randomness or a channel with possible overbank deposits overlaid by two younger layers that can be traced back (ESP\_026162\_2020). (d, e) Schematics of a longitudinal cross-section showing how back-stepping and down-stepping might have occurred during lake-level rise or the lake-level fall.



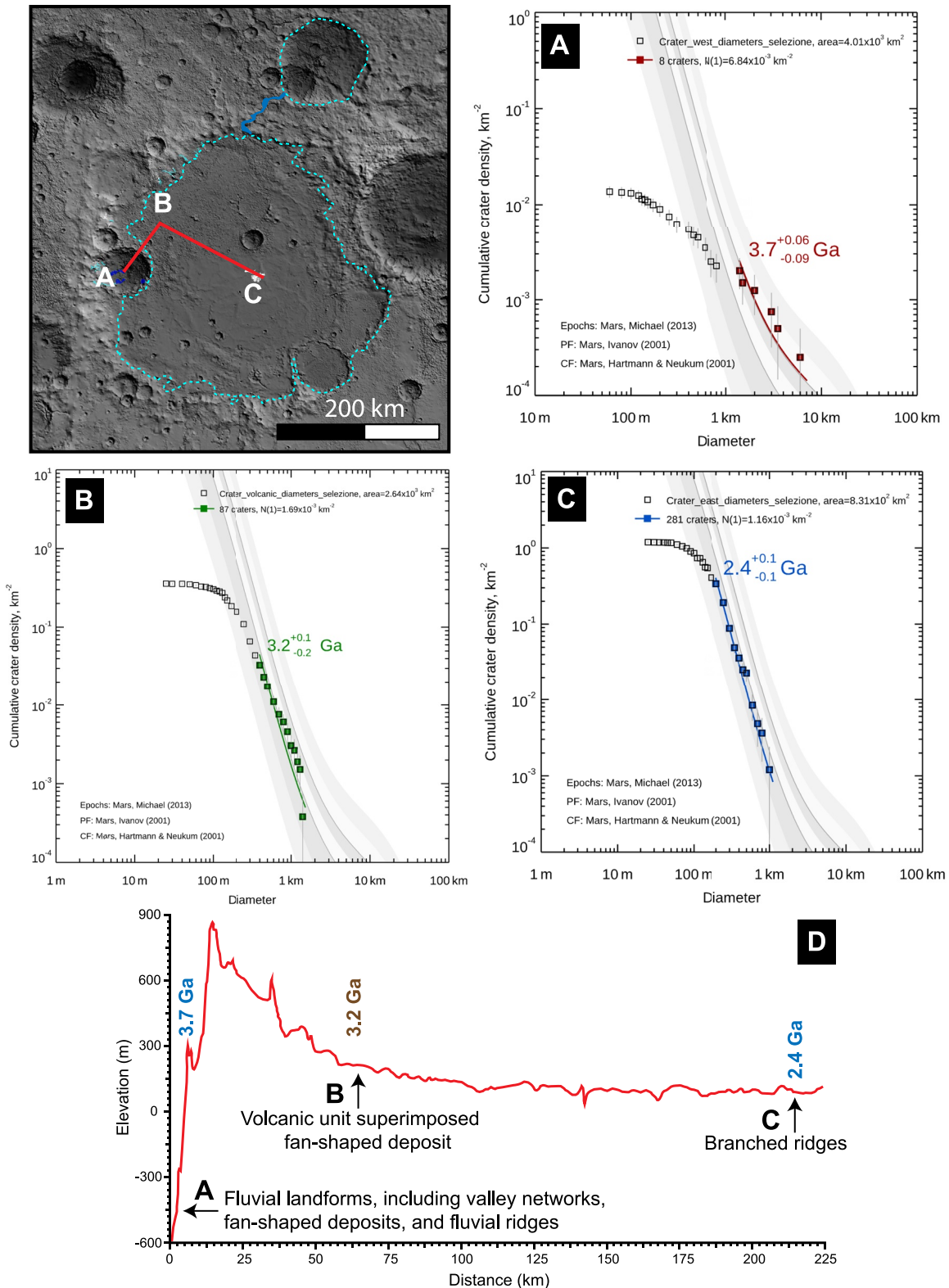


**Figure 8.** A key map showing main sites that have been dated using crater counting. (a) Crater count of craters superposing the fluvial landforms within the unnamed crater shows the best fit to the  $3.7 \pm 0.1$  Ga for the second major interval of the fluvial activity (see Figure S3 in Supporting Information S1). (b) The age of the volcanic unit that superimposes a fan-shaped deposit sourced from the western rim of Antoniadi crater (Figure S4 in Supporting Information S1). (c) Plots of the cumulative size-frequency distribution of craters on the branched ridges with the fitted model age show that the third interval must be older than 2.4 Ga (Figure S5 in Supporting Information S1). (d) Cross section shows the elevation and the geologic units evolution described in the paper.



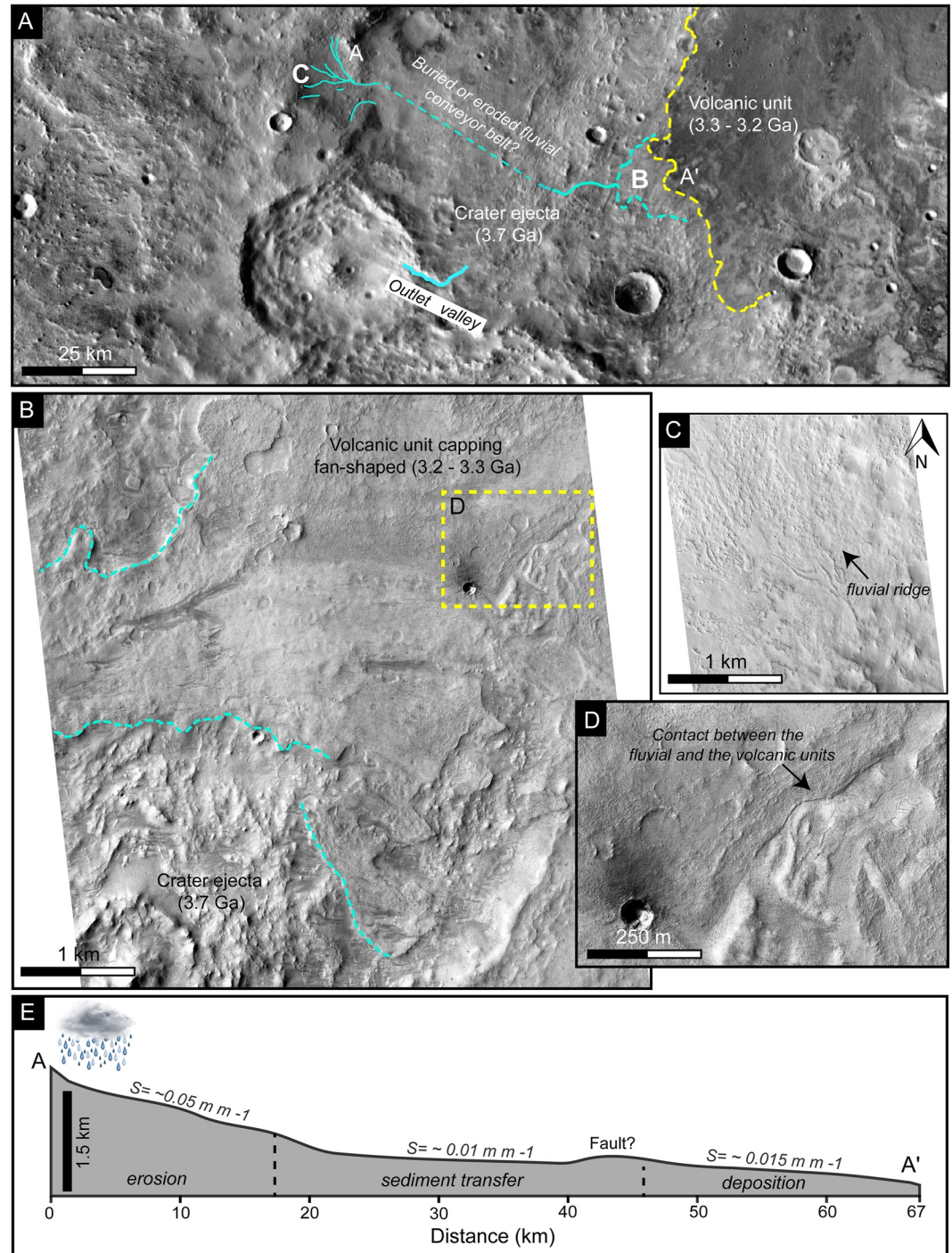


**Figure 9.** A mosaic showing a source-to-sink fluvial system on the western rim of the Antoniadi crater ( $22^{\circ}47'30''\text{N}$ ;  $57^{\circ}48'55''\text{E}$ ). The image shows that a fluvial system overlies crater ejecta that dates back to 3.7 Ga and is capped by a volcanic unit that resurfaced the floor of the Antoniadi crater at 3.3–3.2 Ga. (b–d) Close-up images derived from High-Resolution Imaging Science Experiment showing fluvial ridges in the source zone and fan-shaped deposits in the sink zone. The fan-shaped deposit is capped by a volcanic unit, as seen in portions (b, d) (ESP\_064891\_2030; ESP\_071737\_2025). (e) Profile A-A' of slope changes from the erosion to the deposition zones; the profile was derived from the blended MOLA/HRSC.

arid climate ranges from 0.05 to 0.2. However, this aridity index is a minimum estimate; a higher index could potentially be viable, which means that other climate regimes might have punctuated Antoniadi's geological history.

### 3.1.2. Post-antoniadi Paleolake Fluvial Activity (~3.7 Ga)

Following the filling of the first Antoniadi crater, an unnamed ~65 km-diameter crater was superimposed on the western rim of the first inferred lake within Antoniadi. This superimposition stratigraphically confirms that the fluvial landforms within the ~65 km-diameter must be younger in the first episode. Our CTX, HiRISE, and CaSSIS observations of fluvial and lacustrine landscapes revealed an array of several canyons, three fan-shaped deposits, and fluvial ridges (Figure 6). The canyons are ~1–4 km wide, ~5–15 km long, and have a depth that does not exceed ~300 m. These canyons have a dendritic upstream pattern and connect downstream to main trunks, which would have removed water and sediments, and formed fan-shaped deposits. One of these fans seems to have accumulated at multiple levels as shown in Figure 6, indicating changes in either water level or accommodation. The areas of the fan-shaped deposits range from 23.6 to 47.7 km<sup>2</sup>; tracing the source-to-sink of these fans shows that the water and the sediments were transported from drainage basins with areas roughly ranging from 21 to 324 km<sup>2</sup>. The measured catchment area that might have filled this crater and formed fans does not exceed 2,000 km<sup>2</sup>. The fans accumulated at three distinctive elevations, ranging from ~–1,100 to ~–500 m, suggesting local areas prone to ponding (Figure 6 and Figure S2 in Supporting Information S1). The exposed fluvial sedimentary deposits include sedimentary beds stacked within the fans and contacts between these beds (Figure 6). One of these fan-shaped deposits is connected to a series of valley networks, where the main trunk is in the form of a standing ridge (Figure 7a). The thickness of this ridge-bearing fan ranges from 62 to 127 m and is up to ~1.5 km wide; multiple layers show a channel belt stacking pattern. At the base of the ridge, a ~230-m-wide channel fill is observed with possible lateral deposits, overlain by down-lapping layers that show geometric evidence for either back-stepping (possibly recording a transgression?) (Figures 7b–7d), or a down-stepping due to a fall in the lake level (Figure 7e). Our crater size-frequency data show an age of ~3.7 Ga (late Noachian) for the fluvial deposits accumulated within the crater; this suggests that the crater must be of the same age or older (Figures 4 and 8).

### 3.1.3. Pre-Volcanism Fluvial Activity (~3.7–3.2 Ga)

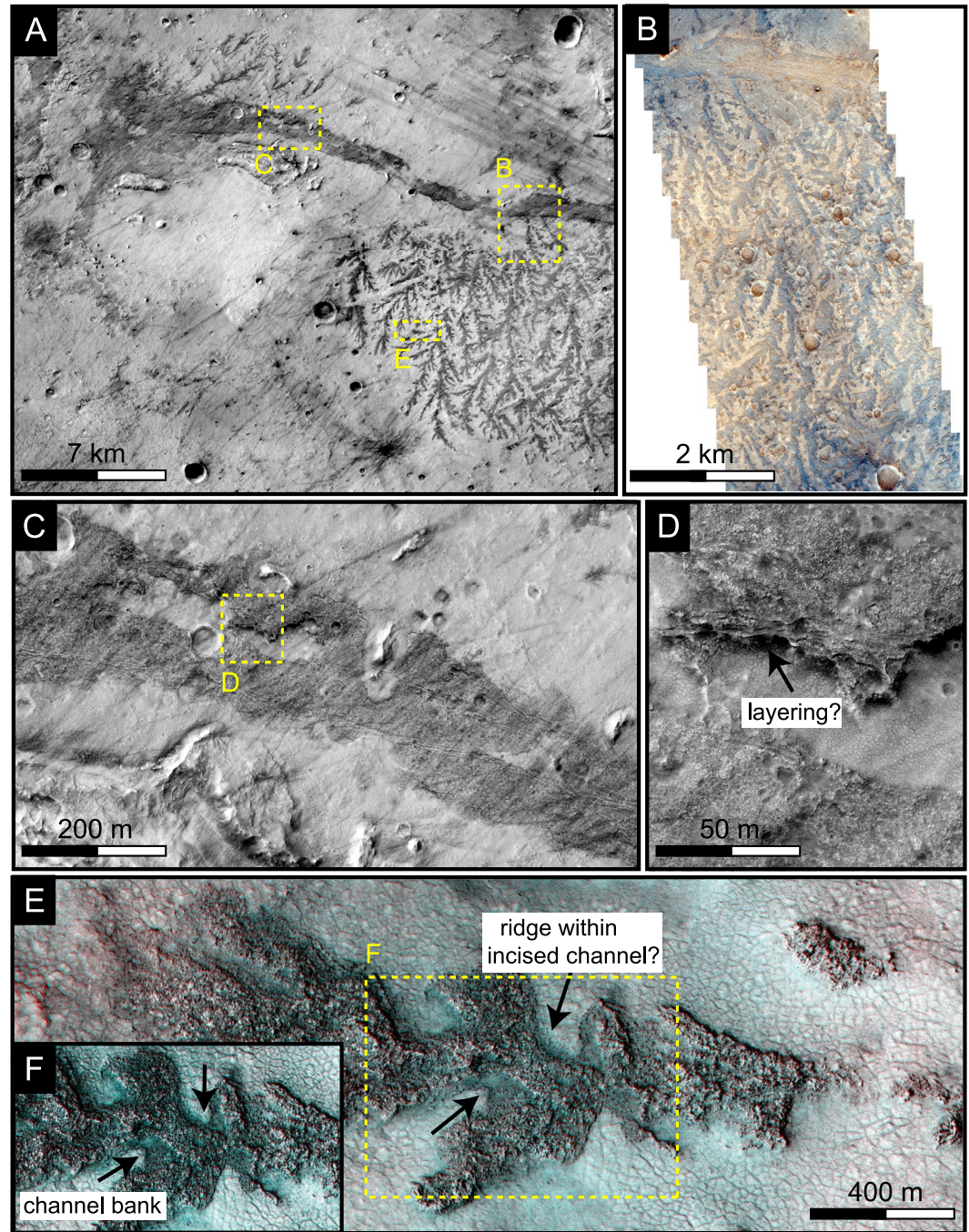
The northwestern rim of Antoniadi crater exhibits numerous fossil fluvial systems that were locally incised into an early Noachian bedrock over an area of 5,000 km<sup>2</sup> (Figure 9). These systems were subsequently transported above the previous crater's ejecta that dated back to ~3.7 (Figure 8). They ranged from single-thread to branching channel patterns (Figure 8) and presumably captured water and sediments at elevations of ~1,850 m and terminated in the crater at elevations of ~600 and ~250 m. Those channels terminate at ~250 m, leaving a fan-shaped deposit that is superimposed by a volcanic unit, limiting the age of this episode to occur between 3.7 and 3.2 Ga (Figure 8).

Southwest of the fan, there is a ~33-km diameter crater that shows a relatively fresh ejecta texture compared to its surroundings dropping into the crater that dated back to ~3.7 Ga, reflecting at least a younger age than the one dated back to 3.7 Ga. We did not observe any complex fluvial features except an outlet valley (Figure 6a; Figure S6 in Supporting Information S1). There is a clear absence of any catchment area. However, filling a lake to the breach level (945 m) likely formed a body of water with an area of nearly 500 km<sup>2</sup> (Figure S6 in Supporting Information S1).

### 3.1.4. Late-Stage Fluvial Activity (~3.2–2.4 Ga)

A suite of broad, dark-toned, multi-branched ridges (dendritic pattern) exists near the Antoniadi basin center (Figure 10). These fine-scale ridges closely approach, and in some cases connect to, a larger ridge that separated the two ridge systems (the southern system and the northern system). Using a HiRISE DEM, we found ridges 1–5 m high and have widths ranging from tens to a few hundred meters with lengths less than 9 km. However, the large ridge is nearly 1 km wide and ~20 km long. The large ridge currently slopes toward the west (Figure 11). However, the present-day slope is likely affected by the existence of major faults and a prominent ridge-resembling wrinkle ridge system, as shown in Figure 11. A CTX DEM shows that the ridge network (former streams) originated from relatively elevated topography in the north and met at a confluence in the main ridge (former trunk valley?) (Figure 8). However, the dendritic ridges in the south run opposite the slope (Figure 11). A

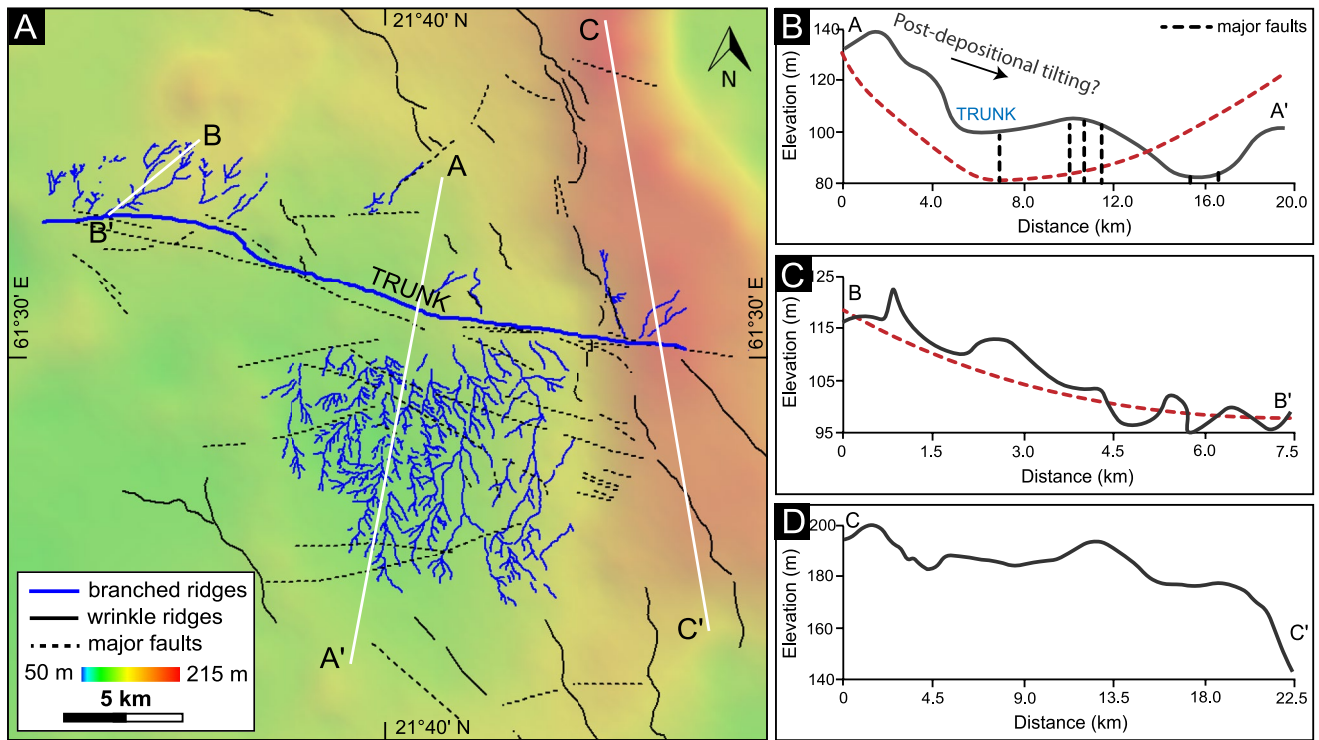




**Figure 10.** An array of short and stubby branched ridges. (a) A set of branched ridges preserve former channels. The tributary generally followed toward a larger, central trunk, which currently slopes toward the west side (CTX; P15\_007095\_2017\_XL\_21N299W). (b) A portion of CaSSIS color image (MY35\_013494\_159\_0) shows the branched ridges. (c, d) High-Resolution Imaging Science Experiment close-up of the central trunk showing layering within the ridge (ESP\_034311\_2020). (e, f) 3D anaglyph close-up portions of a branched ridge. It is clear that the ridges stand within a paleochannel (HiRISE; ESP\_012435\_2015).

wrinkle ridge system occurs toward the south, and thus the southern branched ridge system might have run to the opposite because of post-depositional NE tilting (tectonic?) (Figure 11; Figure S7 in Supporting Information S1). The HiRISE Anaglyph stereo pair reveals that many ridges stand in negative relief that resembles paleo-channels that did not form along with the current topography (Figure 10). Some exposed portions of the primary trunk





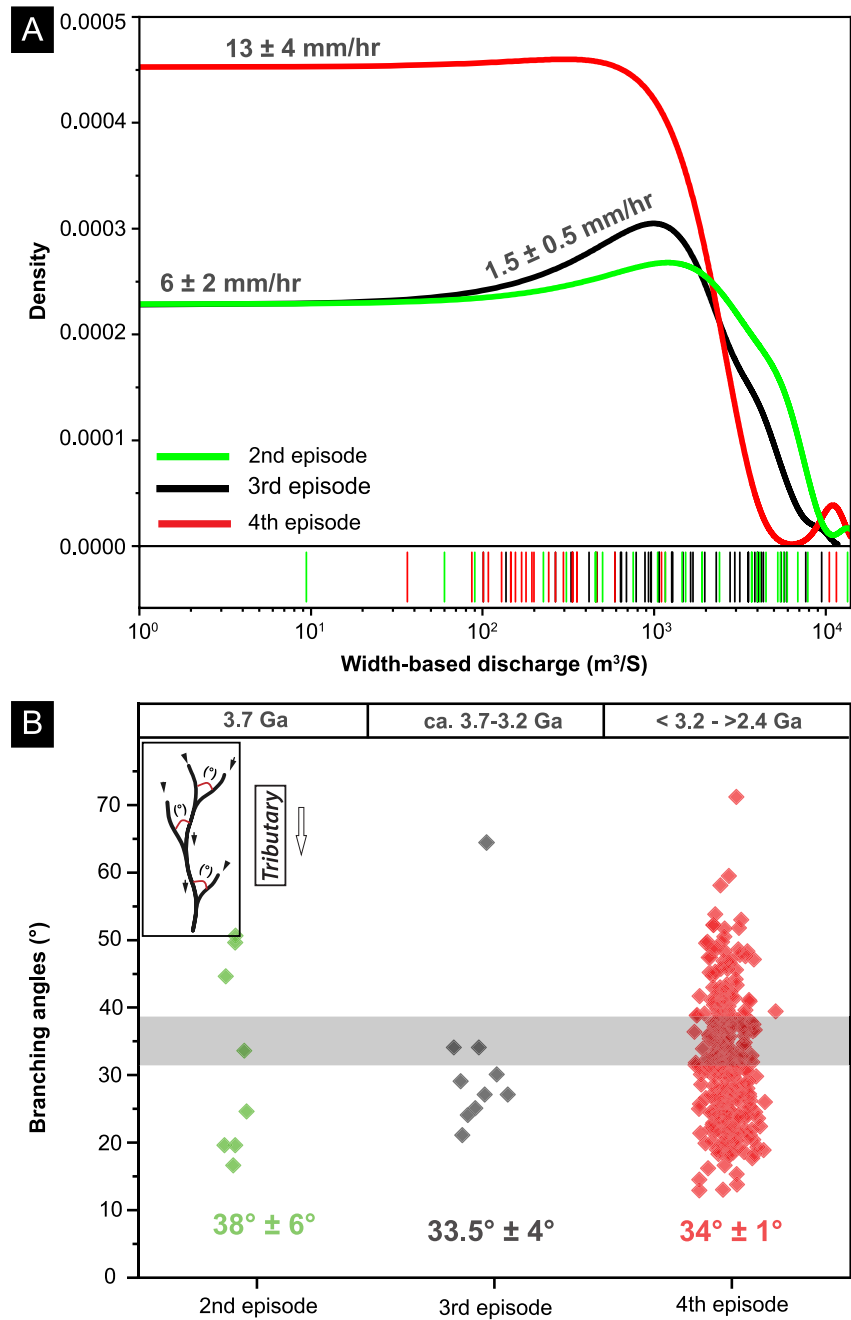
**Figure 11.** (a) Map of the branched ridges, wrinkle ridges, and major faults overlaid on the blended MOLA/HRSC mosaic shows that the drainage network is topographically confined, representing tributary systems on both sides (south and north). Then, they drained into a central trunk. (b) Profile A-A' of slope along the drainage system suggests that tectonic/volcanic uplifts mainly control the system. The red dotted line simply represents the proposed paleo-topographic profile. (c) B-B' profile shows the slope of the branched ridges northern the main trunk. This profile is consistent with the scenario of a tributary drainage system, shown the idea that the ridges south of the main trunk might have tilted after the formation. The red dotted profile shows the idealized fluvial profile. (d) C-C' longitudinal profile of the wrinkle ridge system shows how the slope increases in the north and drops down in the south. Such a profile suggests that a post-depositional NE-tilting might have taken place in the region.

exhibit meter-scale layering within the ridge (Figure 10). The ridges are made up of blocks that are up to 6 m in diameter. Taken together, these observations lead to the conclusion that networks might have formed in response to surface runoff.

Impact crater size-frequency statistics of the unit of the branched ridges (Figure 8) indicate a 2.4 Ga age (Early Amazonian). This shows that their formation occurred before 2.4 Ga. Given that the branched ridges occur over the ~3.2 Ga-old volcanic unit, they must have formed between 3.2 and 2.4 Ga ago.

### 3.2. Discharge Rates and Junction Angles

Calculations of paleodischarge (Figure 12a) were obtained by combining 94 channel and ridge width measurements from three intervals with an empirical, gravity-corrected width-discharge relationship (Equation 1). The second interval of fluvial activity was found to be more intense than the third episode, with an average discharge of  $(3.03 \pm 0.87) \times 10^3 \text{ m}^3 \text{ s}^{-1}$  based on the measurements of 28 ridges as well as the incised valleys (Table S1 in Supporting Information S1). However, paleodischarge estimates calculated from the widths of 41 fluvial ridges formed during the first fluvial interval range from  $(1.01 \pm 0.03) \times 10^3$  to  $(7.6 \pm 2.2) \times 10^3 \text{ m}^3 \text{ s}^{-1}$ , with an average of  $(2.3 \pm 0.67) \times 10^3 \text{ m}^3 \text{ s}^{-1}$  (Table S1 in Supporting Information S1). The last interval was found to have a lower discharge but from a smaller drainage area, with an average of  $(1.12 \pm 0.34) \times 10^3 \text{ m}^3 \text{ s}^{-1}$  determined from 26 width measurements (Table S1 in Supporting Information S1). Dividing the mean discharge of each interval by the rough estimate of the whole catchment area forming that interval gives us a rough estimate of the runoff production, which ranges from 1.5 mm/hr for the second interval to 13 mm/hr for the fourth interval. These estimates are subject to be over-estimated if they preserve channel belts and not channel fill, in which they record lateral migration and vertical aggradation built over a significant geological time (e.g., Dong & Goudge, 2022; Hayden, Lamb, & Carney, 2021).



**Figure 12.** (a) A kernel density estimate (smoothing parameter) of width-discharge rates calculated from three major episodes of fluvial systems within the Antoniadi crater. When dividing the mean channel-forming discharge of each episode by the drainage area leads to the runoff production. (b) Plots of 300 measured junctions from the three intervals showed that the mean for these intervals ranging from  $34^\circ \pm 1^\circ$  to  $38^\circ \pm 6^\circ$ .

A regional survey of the branching angles from  $\sim 300$  tributary streams at Antoniadi crater shows that the junctions from the three intervals range from  $33.5^\circ$  to  $38^\circ$  (Figure 12b). Although the valley networks that formed during these three fluvial intervals span a significant period of geological time and are located on a wide range of slopes ranging from crater rims to vast plains, their junction angles differ only slightly, with variations of  $\sim 5^\circ$  (Figure 12b). This supports the idea that the slope might not significantly change the junction angles.



#### 4. Discussion

Our results place new regional constraints on the hydro-climate history of Antoniadi crater, the site of a potential, persistent, large lake on early Mars; as such, our results provide new insights into the nature and timing of early Martian hydroclimate. Four major fluvial intervals identified here are interpreted to have involved locally sourced fluids and may have developed under episodic conditions over significant geological time, suggesting that the early Martian climate was episodically warm enough to sustain the fluvial activity. This may have been accomplished either by snow melting, rainfall, or groundwater-fed surface runoff on the planet's surface during its early history (Noachian to Hesperian or Early Amazonian) (e.g., Bahia et al., 2022; Cardenas et al., 2022; Carr, 1995, 1996; Davis et al., 2016; Dickson et al., 2020; Grau Galofre et al., 2020; Grotzinger et al., 2015; Hynes et al., 2010; Kite & Noblet, 2022; Kite et al., 2019; Lamb et al., 2006; Malin & Edgett, 2003; Mangold et al., 2021a; Salese et al., 2019; Williams et al., 2013). Our geomorphic observations suggest multiple episodes of fluvial activity within Antoniadi crater, likely driven by several warming events. Nevertheless, these observations do not conclusively establish the atmospheric conditions that would have facilitated surface runoff in this region. Our results identify at least three distinct episodes characterized by the presence of an outlet valley, fans, valley networks, and fluvial ridges. These features could be attributed to precipitation events (either rain or snowfall) or subsequent ice melting. The distinct morphological features of the stubby, branched ridges indicate the possible role of groundwater seepage in the formation of the fourth episode.

The absence of any geomorphic remnants of fluvial systems on the rims of Antoniadi hinders our ability to understand the nature of the first fluvial episode that filled and breached the Antoniadi crater during its early growth. However, our observations reveal that the outlet canyon exhibits terrace-like features at two major elevations or inverted cutbank deposits (Figure 5), implying that its incision occurred over at least two stages during periods of higher standing water levels (Fassett & Head, 2008a; Goudge & Fassett, 2018; Goudge et al., 2018; Gupta et al., 2017). The stratigraphic relationships suggest that this interval must have occurred before  $\sim 3.7$  Ga (i.e., the age of the second episode); it was likely to have occurred between  $\sim 3.81$  and  $3.74$  Ga, which is the age of the oldest-known valley networks in Syrtis Major Planum (e.g., Fassett & Head, 2008b; Jaumann et al., 2010). Together, these observations may indicate multiple hydrologic cycles driven by episodic high-energy flooding, which is consistent with recent observations from the rover at Jezero crater (Mangold et al., 2021a); orbiter data suggest that this may have been a global occurrence (e.g., Goudge et al., 2021; Grau Galofre et al., 2020; Hughes et al., 2019). The volume/area relationship suggests that the watershed required to fill and breach the raised crater rim is  $\sim 550,000$  km<sup>2</sup> (Fassett & Head, 2008a); however, we could not trace any relics of this watershed, emphasizing the role of either erosion or burial in the reconstruction of the early Martian paleo-morphology. This is also consistent with our mapping of fluvial ridges and eroded craters.

The preservation of the structures formed during the second fluvial episode is much better than in the first episode, allowing us to observe sedimentary structures, which include the layering within fans, channels stacked within the fans, possible overbank deposits, and back- or down-stepping sedimentation patterns associated with these fans (Figures 6 and 7). Furthermore, we observed layering within the crater rim that could reflect the lacustrine deposition (Figures 6 and 7). Our age model affirms that the fluvial systems were active  $\sim 3.7$  Ga and peaked runoff around the time of the Noachian-Hesperian boundary (e.g., Davis et al., 2016; Dickson et al., 2020; Fassett & Head, 2008b; Kite et al., 2019; Mangold et al., 2004). The observations of lake-level fluctuations recorded by the deposition of fan-shaped deposits support the conclusion that these features were likely formed within a body of standing water. The basin topography and the fans observed at multiple elevations suggest that the base level of this water body changed over time (Figure 13), which is consistent with a scenario that involves the episodic formation of sedimentary structures associated with fluctuations in the water body. Such a scenario was recently proposed based on in situ observations at the Jezero crater and from orbiter data (e.g., Davis et al., 2018; Grau Galofre et al., 2020; Hughes et al., 2019; Mangold et al., 2021a; Vijayan et al., 2020). The elevation of these fans indicates that the lake within the crater could have exhibited up to three distinct water levels during its formation, as for the Gale crater (Palucis et al., 2016).

At the center of the Antoniadi crater, we interpreted a set of short and stubby branched ridges to be former channels inverted in the modern landscape using differential erosion processes. The short and stubby channels usually form by groundwater sapping, similar to those formed on Earth (e.g., Schumm et al., 1995). This interpretation is based on our observations that include the network organization, possible layering, and the remnants of a paleo-channel in negative relief (Figures 10 and 11). This interpretation is inconsistent with recent studies that proposed

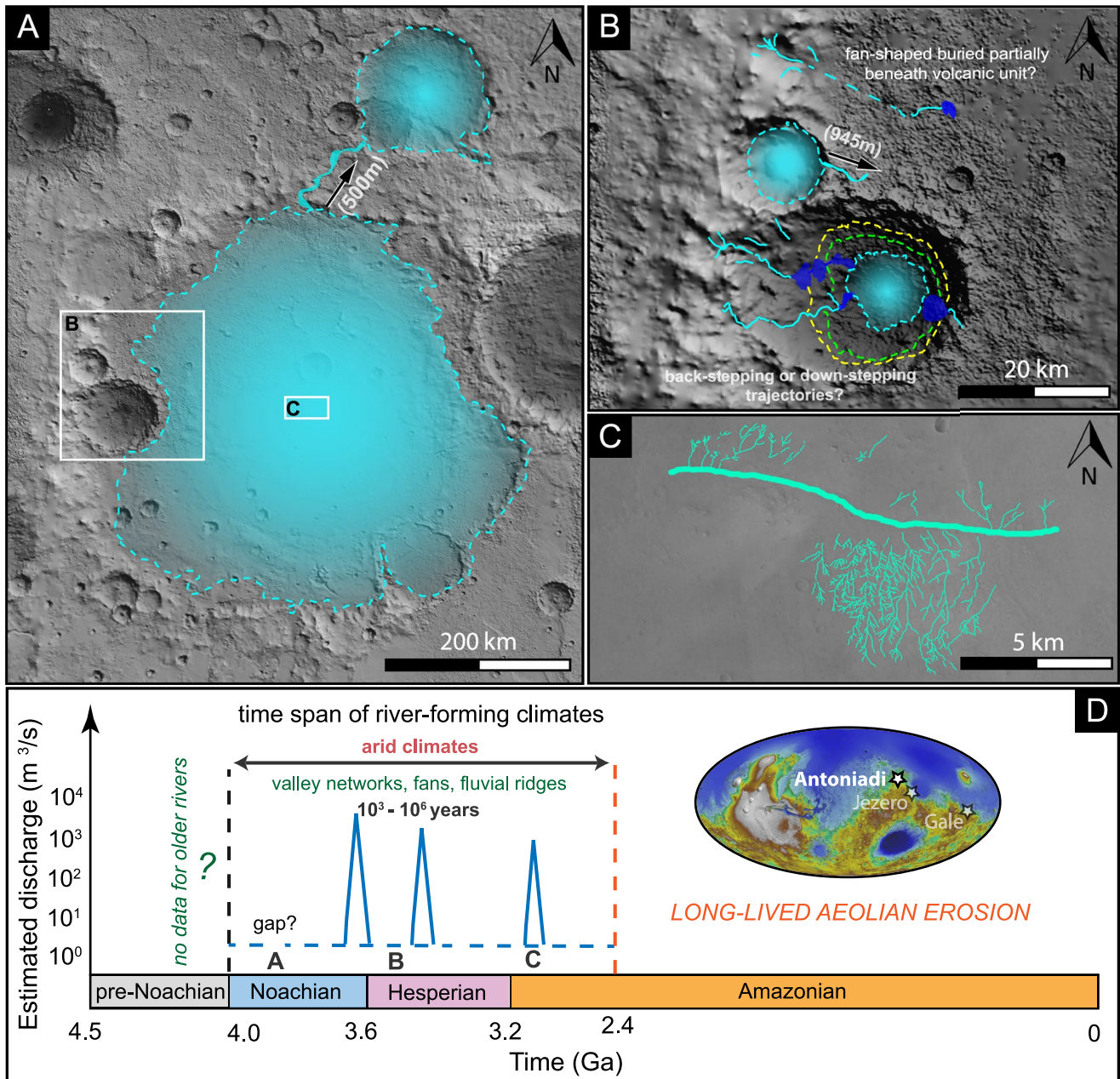


**Figure 13.** The Antoniadi fluvial system's primary growth phases. (a) The inferred paleolake level inside the Antoniadi crater at the time of the formation of the northern outlet canyon, when the lake likely breached the rims during catastrophic floods, forming an outlet canyon at an elevation of  $\sim 500$  m. The lake boundary is tentative and subject to uncertainty, considering the influence of burial and erosion in modifying the Antoniadi basin. The first episode was likely before 3.7 Ga. (b) A new paleolake was recognized based on three fan-shaped deposits, and layering possibly records a lacustrine environment, which was possibly active at  $\sim 3.7$  Ga. Based on the elevations of the fan-shaped deposits, we propose three lake levels ( $\sim 1,100$ ,  $\sim 700$ , and  $\sim 500$  m). North of the paleolake; (1) a crater that was filled and breached at an elevation of 945 m, (2) and a source-to-sink fluvial system that is currently capped by a volcanic unit. These fluvial features could have been formed between 3.7 and 3.2 Ga. The shaded relief topographic maps in (a) and (b) derived from the blended MOLA/HRSC gridded topographic map. (c) In Antoniadi's center, there is a set of branched ridges that we interpret as ancient streams. The background was derived from CTX. These ridges might have formed at some point between 3.2 and 2.4 Ga. (d) A geologic time history of Antoniadi shows the estimated discharge, duration, and climatic regime.

that these branched ridges might have been formed by viscous flows (Mangold et al., 2021b). This mechanism does not create such a network organization (Figures 10 and 11), in contrast to fluvial channels. The formation of these networks by groundwater seepage likely required a warm and wet climate since it is not common to release groundwater in a cold climate (e.g., Abotalib & Heggy, 2019; Tosca et al., 2018). Also, the presence of fractures and faults likely played an important role in triggering the groundwater release. Subsequently, it is possible that



viscous or volcanic flows filled them (Mangold et al., 2021b), making them more resistant to differential erosion to appear as ridges in the modern landscape.

The minimal thickness of the fluvial systems dated back to the second and fourth intervals allows us to provide rough estimates for the minimum duration of the fluvial environments that persisted within the Antoniadi crater. Given the 62–127 m from the fluvial ridges and fans of the second interval, a minimum duration of 0.181–1.26 Ma is obtained, assuming a mean sediment aggradation rate of 0.01–0.7 m/ka (Colombera et al., 2015). Applying the same approach to the third interval yields a minimum duration of 1.4–100 ka. Fluvial sediment accumulation rates can vary significantly by at least 11 orders of magnitude (Sadler, 1981; Sadler & Jerolmack, 2014); hence, the estimated duration was modified to fall within a range of  $10^3$ – $10^6$  years, excluding the dry intervals. Our duration estimates align with previous studies of Mars' fluvial deposits (Balme et al., 2020; Cardenas et al., 2022; Hayden, Lamb, & McElroy, 2021; Lapôtre & Ielpi, 2020; Salese et al., 2020; Stucky de Quay et al., 2019, 2021).

The climatic regime can be inferred from the channel angles of the valley networks (Cang & Luo, 2019; Seybold et al., 2018). Our measurements show that the mean junction angles for each of the three intervals are between 33.5° and 38° (Figure 12), similar to those observed in arid zones on Earth (Seybold et al., 2018). This suggests that three of four intervals of fluvial activity were preserved and expressed at the Martian surface in the Antoniadi crater formed under an arid climate. This suggestion is congruent with the minimum aridity index calculated from the paleolake morphometry, which yields an estimate of the aridity index at 0.18. These suggestions are aligned with a planetwide analysis of Martian valley networks (Cang & Luo, 2019; Seybold et al., 2018) and paleolakes (Stucky de Quay et al., 2020). However, the aridity index derived from lake morphometry could be minimal, considering the role of exhumation and burial in shaping the present-day Antoniadi paleo-lake morphometry. Therefore, there is a possibility that there was a more humid past with either snow melting or rainfall-fed surface runoff that was responsible for filling those lakes.

Many studies have previously reported upon observations that suggest that early Mars might have had climate conditions that could sustain rivers and lakes (e.g., Baker, 2001; Carr, 1995; Davis et al., 2016; Grotzinger et al., 2015; Kite et al., 2019; Malin & Edgett, 2003; Mangold et al., 2021a; Williams et al., 2013; Wilson et al., 2021). The fluvial systems at the Antoniadi crater have allowed us to assess the stratigraphic relationship between the four major episodes of fluvial activity capable of forming and sustaining two paleolakes (Figure 13). Furthermore, the geometry (width and thickness) of the relic fluvial systems, coupled with the measured junction angles, provide insights into the flow conditions as well as rough estimates of the duration and the climatic regime that persisted at Antoniadi crater during its early history. Together, our observations, measurements, and estimations hint at the existence of long-lived and episodic fluvial processes that persisted under arid conditions on early Mars. Along with other geologic lines of evidence, these findings point to potential episodic warming events that enabled periodic surface runoff events under arid climates.

## 5. Conclusions

The fragmentary archive of fluvial activity at the Antoniadi paleolake suggests that the crater, which is presently a hyper-arid desert, hosted at least two large lakes that persisted intermittently across three fluvial intervals during the late Noachian and Early Hesperian (~3.7–2.4 Ga). Our geomorphic and stratigraphic observations, which included terrace-like forms within the outlet canyon, show that the first interval involved episodic discharges that likely resulted in sustained fluvial activity but were dotted by catastrophic floods that carved the outlet canyon. The preservation of the second interval allowed us to observe multiple valley networks and fluvial ridges accumulating within the crater, forming fans at multiple elevations, recording a back-stepping or down-stepping trajectory, and bearing evidence of lake-level fluctuations. Subsequently, we observed an array of branched ridges and fan-shaped deposits that are stratigraphically distinct, supporting episodic surface runoff, which continued after the formation of the first two intervals. The climatic regime and discharge flow rates were constrained by the geometries of the fluvial systems, implying prolonged riverine processes over the course of thousands to millions of years under arid climates. Overall, our results support the hypothesis that episodic warming punctuated the climate of early Mars, better elucidating the apparent paradox of flowing water on a now-frozen planet.

## Data Availability Statement

The following standard data products mentioned in the manuscript are freely accessible via NASA Planetary Data Systems. (a) CTX (Malin, 2007). (b) HiRISE (McEwen, 2007). (c) MOLA (Fergason et al., 2018; Neumann et al., 2003). (d) CaSSIS: CaSSIS data are available through the ESA Planetary Science Archive (accessed CaSSIS, 2023). DTMs, measurements, and calculations are archived/achieved in Zaki (2022).

## Acknowledgments

This research was funded by a Swiss Confederation Ph.D. Grant (Nr: 2017.1006) to Abdallah S. Zaki. Additional funding came from the Department of Earth Sciences, University of Geneva. Abdallah Zaki thanks Caleb Fassett, Robin Wordsworth, Luis Valero, and Solmaz Adelia for the helpful discussion about the Antoniadi crater, early Mars climate models, and age models. We thank Bradley Thomson for handling the manuscript. The manuscript has benefited from the constructive comments of Rickbir S. Bahia, Vijayan S, and an anonymous reviewer. This study has been supported by the Italian Space Agency (ASI-INAF agreement no. 2020-17-HH.0). The authors wish to thank the ExoMars spacecraft and CaSSIS instrument engineering teams for the successful completion of the instrument. CaSSIS is a project of the University of Bern and funded through the Swiss Space Office via ESA PRODEX programme. The instrument hardware development was also supported by the Italian Space Agency (ASI) (ASI-INAF agreement no. 2020-17-HH.0), INAF/Astronomical Observatory of Padova, and the Space Research Center (CBK) in Warsaw. Support from SGF (Budapest), the University of Arizona (Lunar and Planetary Lab.) and NASA are also gratefully acknowledged. Operations support from the UK Space Agency under grant ST/R003025/1 is also acknowledged. E.S.K. acknowledges support from NASA (80NSSC20K0144). Open access funding provided by Universite de Geneve.

## References

- Abotaleb, A. Z., & Heggy, E. (2019). A deep groundwater origin for recurring slope lineae on Mars. *Nature Geoscience*, *12*(4), 235–241. <https://doi.org/10.1038/s41561-019-0327-5>
- Bahia, R. S., Covey-Crump, S., Jones, M. A., & Mitchell, N. (2022). Discordance analysis on a high-resolution valley network map of Mars: Assessing the effects of scale on the conformity of Valley Orientation and surface slope direction. *Icarus*, *383*, 115041. <https://doi.org/10.1016/j.icarus.2022.115041>
- Baker, V. R. (2001). Water and the Martian landscape. *Nature*, *412*(6843), 228–236. <https://doi.org/10.1038/35084172>
- Balme, M. R., Gupta, S., Davis, J. M., Fawdon, P., Grindrod, P. M., Bridges, J. C., et al. (2020). Aram Dorsum: An extensive mid-Noachian age fluvial depositional system in Arabia Terra, Mars. *Journal of Geophysical Research: Planets*, *125*(5), e2019JE006244. <https://doi.org/10.1029/2019je006244>
- Cabrol, N., & Grin, E. A. (1999). Distribution, classification, and ages of Martian impact crater lakes. *Icarus*, *142*(1), 160–172. <https://doi.org/10.1006/icar.1999.6191>
- Cang, X., & Luo, W. (2019). Noachian climatic conditions on Mars inferred from valley network junction angles. *Earth and Planetary Science Letters*, *526*, 115768. <https://doi.org/10.1016/j.epsl.2019.115768>
- Cardenas, B. T., Lamb, M. P., & Grotzinger, J. P. (2022). Martian landscapes of fluvial ridges carved from ancient sedimentary basin fill. *Nature Geoscience*, *15*(11), 871–877. <https://doi.org/10.1038/s41561-022-01058-2>
- Cardenas, B. T., Mohrig, D., & Goudge, T. A. (2017). Fluvial stratigraphy of valley fills at Aeolis Dorsa, Mars: Evidence for base-level fluctuations controlled by a downstream water body. *GSA Bulletin*, *130*(3–4), 484–498. <https://doi.org/10.1130/b31567.1>
- Carr, M. H. (1995). The Martian drainage system and the origin of valley networks and fretted channels. *Journal of Geophysical Research*, *100*(E4), 7479. <https://doi.org/10.1029/95je00260>
- Carr, M. H. (1996). Channels and valleys on Mars: Cold climate features formed as a result of a thickening cryosphere. *Planetary and Space Science*, *44*(11), 1411–1423. [https://doi.org/10.1016/s0032-0633\(96\)00053-0](https://doi.org/10.1016/s0032-0633(96)00053-0)
- CaSSIS. (2023). CaSSIS data are available through the ESA Planetary Science Archive. Retrieved from <http://archives.esac.esa.int/psa/#!Table%20View/CaSSIS=instrument>
- Castelltort, S., Simpson, G., & Darrioulat, A. (2009). Slope-control on the aspect ratio of river basins. *Terra Nova*, *21*(4), 265–270. <https://doi.org/10.1111/j.1365-3121.2009.00880.x>
- Castelltort, S., & Yamato, P. (2013). The influence of surface slope on the shape of river basins: Comparison between nature and numerical landscape simulations. *Geomorphology*, *192*, 71–79. <https://doi.org/10.1016/j.geomorph.2013.03.022>
- Colombera, L., Mountney, N. P., & McCaffrey, W. D. (2015). A meta-study of relationships between fluvial channel-body stacking pattern and aggradation rate: Implications for sequence stratigraphy. *Geology*, *43*(4), 283–286. <https://doi.org/10.1130/g36385.1>
- Davis, J. M., Balme, M., Grindrod, P. M., Williams, R. M. E., & Gupta, S. (2016). Extensive Noachian fluvial systems in Arabia Terra: Implications for early Martian climate. *Geology*, *44*(10), 847–850. <https://doi.org/10.1130/g38247.1>
- Davis, J. M., Grindrod, P. M., Fawdon, P., Williams, R. M., Gupta, S., & Balme, M. (2018). Episodic and declining fluvial processes in southwest Melas Chasma, Valles Marineris, Mars. *Journal of Geophysical Research: Planets*, *123*(10), 2527–2549. <https://doi.org/10.1029/2018je005710>
- Davis, J. M., Gupta, S., Balme, M., Grindrod, P. M., Fawdon, P., Dickeson, Z. L., & Williams, R. M. E. (2019). A diverse array of fluvial depositional systems in Arabia Terra: Evidence for mid-Noachian to early Hesperian rivers on Mars. *Journal of Geophysical Research: Planets*, *124*(7), 1913–1934. <https://doi.org/10.1029/2019je005976>
- De Blasio, F. V. (2022). The large dendritic morphologies in the Antoniadi Crater (Mars) and their potential astrobiological significance. *Geosciences*, *12*(2), 53. <https://doi.org/10.3390/geosciences12020053>
- Devauchelle, O., Petroff, A. P., Seybold, H. F., & Rothman, D. H. (2012). Ramification of stream networks. *Proceedings of the National Academy of Sciences*, *109*(51), 20832–20836. <https://doi.org/10.1073/pnas.1215218109>
- Dickson, J. L., Lamb, M. P., Williams, R. M. E., Hayden, A. T., & Fischer, W. W. (2020). The global distribution of depositional rivers on early Mars. *Geology*, *49*(5), 504–509. <https://doi.org/10.1130/g48457.1>
- Dietrich, W. E., Palucis, M. C., Williams, R. M., Lewis, K. W., Rivera-Hernandez, F., & Sumner, D. Y. (2017). Fluvial gravels on Mars. *Gravel-Bed Rivers*, 755–783. <https://doi.org/10.1002/9781118971437.ch28>
- Dong, T. Y., & Goudge, T. A. (2022). Quantitative relationships between river and channel-belt planform patterns. *Geology*, *50*(9), 1053–1057. <https://doi.org/10.1130/g49935.1>
- Eaton, B. C. (2013). 9.18 hydraulic geometry: Empirical investigations and theoretical approaches. *Treatise on Geomorphology*, 313–329. <https://doi.org/10.1016/b978-0-12-374739-6.00243-8>
- El Maarry, M. R., Markiewicz, W. J., Mellon, M. T., Goetz, W., Dohm, J. M., & Pack, A. (2010). Crater floor polygons: Desiccation patterns of ancient lakes on Mars? *Journal of Geophysical Research*, *115*(E10), E10006. <https://doi.org/10.1029/2010je003609>
- Fassett, C. I., & Head, J. W. (2008a). The timing of Martian Valley network activity: Constraints from buffered crater counting. *Icarus*, *195*(1), 61–89. <https://doi.org/10.1016/j.icarus.2007.12.009>
- Fassett, C. I., & Head, J. W. (2008b). Valley network-fed, open-basin lakes on Mars: Distribution and implications for Noachian surface and subsurface hydrology. *Icarus*, *198*(1), 37–56. <https://doi.org/10.1016/j.icarus.2008.06.016>
- Fergason, R. L., Hare, T. M., & Laura, J. (2018). *HRSC and MOLA blended digital elevation model at 200 m v2*. Astrogeology PDS Annex, U.S. Geological Survey. Retrieved from [http://bit.ly/HRSC\\_MOLA\\_Blend\\_v0](http://bit.ly/HRSC_MOLA_Blend_v0)
- Goudge, T. A., Aureli, K. L., Head, J. W., Fassett, C. I., & Mustard, J. F. (2015). Classification and analysis of candidate impact crater-hosted closed-basin lakes on Mars. *Icarus*, *260*, 346–367. <https://doi.org/10.1016/j.icarus.2015.07.026>
- Goudge, T. A., & Fassett, C. I. (2018). Incision of Licus Vallis, Mars, from multiple lake overflow floods. *Journal of Geophysical Research: Planets*, *123*(2), 405–420. <https://doi.org/10.1002/2017je005438>



- Goudge, T. A., Fassett, C. I., Head, J. W., Mustard, J. F., & Aureli, K. L. (2016). Insights into surface runoff on early Mars from paleolake basin morphology and stratigraphy. *Geology*, *44*(6), 419–422. <https://doi.org/10.1130/g37734.1>
- Goudge, T. A., Mohrig, D., Cardenas, B. T., Hughes, C. M., & Fassett, C. I. (2018). Stratigraphy and paleohydrology of delta channel deposits, Jezero Crater, Mars. *Icarus*, *301*, 58–75. <https://doi.org/10.1016/j.icarus.2017.09.034>
- Goudge, T. A., Morgan, A. M., Stucky de Quay, G., & Fassett, C. I. (2021). The importance of Lake breach floods for valley incision on early Mars. *Nature*, *597*(7878), 645–649. <https://doi.org/10.1038/s41586-021-03860-1>
- Grau Galofre, A., Bahia, R. S., Jellinek, A. M., Whipple, K. X., & Gallo, R. (2020). Did Martian Valley Networks substantially modify the landscape? *Earth and Planetary Science Letters*, *547*, 116482. <https://doi.org/10.1016/j.epsl.2020.116482>
- Grotzinger, J. P., Gupta, S., Malin, M. C., Rubin, D. M., Schieber, J., Siebach, K., et al. (2015). Deposition, exhumation, and paleoclimate of an ancient lake deposit, Gale Crater, Mars. *Science*, *350*(6257), aac7575. <https://doi.org/10.1126/science.aac7575>
- Gupta, S., Collier, J. S., Garcia-Moreno, D., Oggioni, F., Trentesaux, A., Vanneste, K., et al. (2017). Two-stage opening of the Dover strait and the origin of Island Britain. *Nature Communications*, *8*(1), 15101. <https://doi.org/10.1038/ncomms15101>
- Hartmann, W. K., & Neukum, G. (2001). Cratering chronology and the evolution of Mars. In *Space sciences series of ISSI* (pp. 165–194). [https://doi.org/10.1007/978-94-017-1035-0\\_6](https://doi.org/10.1007/978-94-017-1035-0_6)
- Hayden, A. T., Lamb, M. P., & Carney, A. J. (2021). Similar curvature-to-width ratios for channels and channel belts: Implications for paleo-hydraulics of fluvial ridges on Mars. *Geology*, *49*(7), 837–841. <https://doi.org/10.1130/G48370.1>
- Hayden, A. T., Lamb, M. P., Fischer, W. W., Ewing, R. C., McElroy, B. J., & Williams, R. M. E. (2019). Formation of sinuous ridges by inversion of river-channel belts in Utah, USA, with implications for Mars. *Icarus*, *332*, 92–110. <https://doi.org/10.1016/j.icarus.2019.04.019>
- Hayden, A. T., Lamb, M. P., & McElroy, B. J. (2021). Constraining the timespan of fluvial activity from the intermittency of sediment transport on Earth and Mars. *Geophysical Research Letters*, *48*(16), e2021GL092598. <https://doi.org/10.1029/2021gl092598>
- Higgins, C. G. (1982). Drainage systems developed by sapping on Earth and Mars. *Geology*, *10*(3), 147. [https://doi.org/10.1130/0091-7613\(1982\)10<147:dsdbs>2.0.co;2](https://doi.org/10.1130/0091-7613(1982)10<147:dsdbs>2.0.co;2)
- Howard, A. D., Moore, J. M., & Irwin, R. P. (2005). An intense terminal epoch of widespread fluvial activity on early Mars: 1. Valley network incision and associated deposits. *Journal of Geophysical Research*, *110*(E12), E12S14. <https://doi.org/10.1029/2005je002459>
- Hughes, C. M., Cardenas, B. T., Goudge, T. A., & Mohrig, D. (2019). Deltaic deposits indicative of a paleo-coastline at Aeolis Dorsa, Mars. *Icarus*, *317*, 442–453. <https://doi.org/10.1016/j.icarus.2018.08.009>
- Hynek, B. M., Beach, M., & Hoke, M. R. (2010). Updated global map of Martian Valley Networks and implications for climate and hydrologic processes. *Journal of Geophysical Research*, *115*(E9), E09008. <https://doi.org/10.1029/2009je003548>
- Irwin, R. P., Howard, A. D., Craddock, R. A., & Moore, J. M. (2005). An intense terminal epoch of widespread fluvial activity on early Mars: 2. Increased runoff and paleolake development. *Journal of Geophysical Research*, *110*(E12), E12S15. <https://doi.org/10.1029/2005je002460>
- Jacobsen, R. E., & Burr, D. M. (2016). Greater contrast in Martian hydrological history from more accurate estimates of paleodischarge. *Geophysical Research Letters*, *43*(17), 8903–8911. <https://doi.org/10.1002/2016gl070535>
- Jacobsen, R. E., & Burr, D. M. (2018). Errors in Martian paleodischarge skew interpretations of hydrologic history: Case study of the Aeolis Dorsa, Mars, with insights from the Quinn River, NV. *Icarus*, *302*, 407–417. <https://doi.org/10.1016/j.icarus.2017.11.014>
- Jaumann, R., Nass, A., Tirsch, D., Reiss, D., & Neukum, G. (2010). The western Libya Montes Valley System on Mars: Evidence for episodic and multi-genetic erosion events during the Martian history. *Earth and Planetary Science Letters*, *294*(3–4), 272–290. <https://doi.org/10.1016/j.epsl.2009.09.026>
- Kirk, R. L., Howington-Kraus, E., Rosiek, M. R., Anderson, J. A., Archinal, B. A., Becker, K. J., et al. (2008). Ultrahigh resolution topographic mapping of Mars with MRO HiRISE stereo images: Meter-scale slopes of candidate Phoenix landing sites. *Journal of Geophysical Research*, *113*, E00A24. <https://doi.org/10.1029/2007je003000>
- Kite, E. S. (2019). Geologic constraints on early Mars climate. *Space Science Reviews*, *215*(1), 10. <https://doi.org/10.1007/s11214-018-0575-5>
- Kite, E. S., Howard, A. D., Lucas, A., & Lewis, K. W. (2015). Resolving the era of river-forming climates on Mars using stratigraphic logs of river-deposit dimensions. *Earth and Planetary Science Letters*, *420*, 55–65. <https://doi.org/10.1016/j.epsl.2015.03.019>
- Kite, E. S., Mayer, D. P., Wilson, S. A., Davis, J. M., Lucas, A. S., & Stucky de Quay, G. (2019). Persistence of intense, climate-driven runoff late in Mars history. *Science Advances*, *5*(3), eaav7710. <https://doi.org/10.1126/sciadv.aav7710>
- Kite, E. S., & Noblet, A. (2022). High and dry: Billion-year trends in the aridity of river-forming climates on Mars. *Geophysical Research Letters*, *49*(24), e2022GL101150. <https://doi.org/10.1029/2022gl101150>
- Kite, E. S., Steele, L. J., Mischna, M. A., & Richardson, M. I. (2021). Warm early Mars surface enabled by high-altitude water ice clouds. *Proceedings of the National Academy of Sciences*, *118*(18), e2101959118. <https://doi.org/10.1073/pnas.2101959118>
- Lamb, M. P., Howard, A. D., Johnson, J., Whipple, K. X., Dietrich, W. E., & Perron, J. T. (2006). Can springs cut canyons into rock? *Journal of Geophysical Research*, *111*(E7), E07002. <https://doi.org/10.1029/2005je002663>
- Lapôtre, M. G., & Ielpi, A. (2020). The pace of fluvial meanders on Mars and implications for the western delta deposits of Jezero Crater. *AGU Advances*, *1*(2), e2019AV000141. <https://doi.org/10.1029/2019av000141>
- Malin, M. C. (2007). MRO Context Camera experiment data record level 0 v1.0 [Dataset]. NASA Planetary Data System. <https://doi.org/10.17189/1520266>
- Malin, M. C., Bell, J. F., Cantor, B. A., Caplinger, M. A., Calvin, W. M., Clancy, R. T., et al. (2007). Context camera investigation on board the Mars Reconnaissance Orbiter. *Journal of Geophysical Research*, *112*(E5), E05S04. <https://doi.org/10.1029/2006je002808>
- Malin, M. C., & Edgett, K. S. (2000). Evidence for recent groundwater seepage and surface runoff on Mars. *Science*, *288*(5475), 2330–2335. <https://doi.org/10.1126/science.288.5475.2330>
- Malin, M. C., & Edgett, K. S. (2003). Evidence for persistent flow and aqueous sedimentation on early Mars. *Science*, *302*(5652), 1931–1934. <https://doi.org/10.1126/science.1090544>
- Mangold, N., Gupta, S., Gasnault, O., Dromart, G., Tarnas, J. D., Sholes, S. F., et al. (2021a). Perseverance rover reveals an ancient delta-lake system and flood deposits at Jezero Crater, Mars. *Science*, *374*(6568), 711–717. <https://doi.org/10.1126/science.abc4051>
- Mangold, N., Quantin, C., Véronique, A., Delacourt, C., & Allemand, P. (2004). Evidence for precipitation on Mars from dendritic valleys in the Valles Marineris area. *Science*, *305*(5680), 78–81. <https://doi.org/10.1126/science.1097549>
- Mangold, N., Tornabene, L., Conway, S. J., Gunimper, A., Noblet, A., Fawdon, P., et al. (2021b). The unexpected origin of the branched ridges at Antoniadi crater, Mars. In *52nd lunar and planetary science conference, #1994*.
- McEwen, A. S. (2007). *Mars reconnaissance orbiter high resolution imaging science experiment, reduced data record, MRO-M-HIRISE-3-RDR-V1.1*. NASA Planetary Data System. <https://doi.org/10.17189/1520303>
- McEwen, A. S., Eliason, E. M., Bergstrom, J. W., Bridges, N. T., Hansen, C. J., Delamere, W. A., et al. (2007). Mars Reconnaissance Orbiter's high resolution imaging science experiment (HiRISE). *Journal of Geophysical Research*, *112*(E5), E05S02. <https://doi.org/10.1029/2005je002605>

- Michael, G. G. (2013). Planetary surface dating from crater size–frequency distribution measurements: Multiple resurfacing episodes and Differential Isochron fitting. *Icarus*, 226(1), 885–890. <https://doi.org/10.1016/j.icarus.2013.07.004>
- Michael, G. G., & Neukum, G. (2010). Planetary surface dating from crater size–frequency distribution measurements: Partial resurfacing events and statistical age uncertainty. *Earth and Planetary Science Letters*, 294(3–4), 223–229. <https://doi.org/10.1016/j.epsl.2009.12.041>
- Neukum, G. (1983). Meteoritenbombardement und Datierung planetarer Oberflächen (dissertation). Munich.
- Neumann, G., Zuber, M., & Smith, D. E. (2003). MOLA mission experiment gridded data record [Dataset]. NASA Planetary Data System. <https://doi.org/10.17189/1519460>
- Palucis, M. C., Dietrich, W. E., Williams, R. M. E., Hayes, A. G., Parker, T., Sumner, D. Y., et al. (2016). Sequence and relative timing of large lakes in Gale crater (Mars) after the formation of Mount Sharp. *Journal of Geophysical Research: Planets*, 121(3), 472–496. <https://doi.org/10.1002/2015je004905>
- Sadler, P. M. (1981). Sediment accumulation rates and the completeness of stratigraphic sections. *The Journal of Geology*, 89(5), 569–584. <https://doi.org/10.1086/628623>
- Sadler, P. M., & Jerolmack, D. J. (2014). Scaling laws for aggradation, denudation and progradation rates: The case for time-scale invariance at sediment sources and sinks. *Geological Society, London, Special Publications*, 404(1), 69–88. <https://doi.org/10.1144/sp404.7>
- Salese, F., McMahon, W. J., Balme, M. R., Ansan, V., Davis, J. M., & Kleinhans, M. G. (2020). Sustained fluvial deposition recorded in Mars' Noachian Stratigraphic record. *Nature Communications*, 11(1), 2067. <https://doi.org/10.1038/s41467-020-15622-0>
- Salese, F., Pondrelli, M., Neeseman, A., Schmidt, G., & Ori, G. G. (2019). Geological evidence of planet-wide groundwater system on Mars. *Journal of Geophysical Research: Planets*, 124(2), 374–395. <https://doi.org/10.1029/2018je005802>
- Schumm, S. A., Boyd, K. F., Wolff, C. G., & Spitz, W. J. (1995). A groundwater sapping landscape in the Florida Panhandle. *Geomorphology*, 12(4), 281–297. [https://doi.org/10.1016/0169-555x\(95\)00011-s](https://doi.org/10.1016/0169-555x(95)00011-s)
- Seybold, H. J., Kite, E., & Kirchner, J. W. (2018). Branching geometry of valley networks on Mars and Earth and its implications for early Martian climate. *Science Advances*, 4(6), eaar6692. <https://doi.org/10.1126/sciadv.aar6692>
- Stack, K. M., Williams, N. R., Calef, F., Sun, V. Z., Williford, K. H., Farley, K. A., et al. (2020). Photogeologic map of the perseverance rover field site in Jezero crater constructed by the Mars 2020 science team. *Space Science Reviews*, 216(8), 127. <https://doi.org/10.1007/s11214-020-00739-x>
- Stucky de Quay, G., Goudge, T. A., & Fassett, C. I. (2020). Precipitation and aridity constraints from paleolakes on early Mars. *Geology*, 48(12), 1189–1193. <https://doi.org/10.1130/g47886.1>
- Stucky de Quay, G., Goudge, T. A., Kite, E. S., Fassett, C. I., & Guzewich, S. D. (2021). Limits on runoff episode duration for early Mars: Integrating lake hydrology and climate models. *Geophysical Research Letters*, 48(15), e2021GL093523. <https://doi.org/10.1029/2021gl093523>
- Stucky de Quay, G., Kite, E. S., & Mayer, D. P. (2019). Prolonged fluvial activity from channel-fan systems on Mars. *Journal of Geophysical Research: Planets*, 124(11), 3119–3139. <https://doi.org/10.1029/2019je006167>
- Tanaka, K. L. (2014). *Geologic map of Mars US Geological Survey scientific investigations map SIM 3292*. United States Geological Survey. Retrieved from <http://pubs.usgs.gov/sim/3292>
- Thomas, N., Cremonese, G., Ziethe, R., Gerber, M., Brändli, M., Bruno, G., et al. (2017). The colour and stereo surface imaging system (CaSSIS) for the ExoMars trace gas orbiter. *Space Science Reviews*, 212(3–4), 1897–1944. <https://doi.org/10.1007/s11214-017-0421-1>
- Tosca, N. J., Ahmed, I. A., Tutolo, B. M., Ashpittel, A., & Hurowitz, J. A. (2018). Magnetite authigenesis and the warming of early Mars. *Nature Geoscience*, 11(9), 635–639. <https://doi.org/10.1038/s41561-018-0203-8>
- Vijayan, S., Sinha, R. K., Harish, & Anilkumar, R. (2020). Evidence for multiple superposed fluvial deposits within Reuyl Crater, Mars. *Journal of Geophysical Research: Planets*, 125(3), e2019JE006136. <https://doi.org/10.1029/2019je006136>
- Warner, N. H., Gupta, S., Calef, F., Grindrod, P., Boll, N., & Goddard, K. (2015). Minimum effective area for high resolution crater counting of Martian terrains. *Icarus*, 245, 198–240. <https://doi.org/10.1016/j.icarus.2014.09.024>
- Williams, R. M. E., Grotzinger, J. P., Dietrich, W. E., Gupta, S., Sumner, D. Y., Wiens, R. C., et al. (2013). Martian fluvial conglomerates at Gale crater. *Science*, 340(6136), 1068–1072. <https://doi.org/10.1126/science.1237317>
- Williams, R. M. E., Irwin, R. P., & Zimbelman, J. R. (2009). Evaluation of paleohydrologic models for terrestrial inverted channels: Implications for application to Martian sinuous ridges. *Geomorphology*, 107(3–4), 300–315. <https://doi.org/10.1016/j.geomorph.2008.12.015>
- Wilson, S. A., Morgan, A. M., Howard, A. D., & Grant, J. A. (2021). The global distribution of craters with alluvial fans and deltas on Mars. *Geophysical Research Letters*, 48(4), e2020GL091653. <https://doi.org/10.1029/2020gl091653>
- Wordsworth, R. D., Kerber, L., Pierrehumbert, R. T., Forget, F., & Head, J. W. (2015). Comparison of “warm and wet” and “cold and icy” scenarios for early Mars in a 3-D climate model. *Journal of Geophysical Research: Planets*, 120, 1201–1219. <https://doi.org/10.1002/2015je004787>
- Wordsworth, R. D., Forget, F., Millour, E., Head, J. W., Madeleine, J.-B., & Charnay, B. (2013). Global modelling of the early Martian climate under a denser CO<sub>2</sub> atmosphere: Water cycle and ice evolution. *Icarus*, 222(1), 1–19. <https://doi.org/10.1016/j.icarus.2012.09.036>
- Wordsworth, R. D., Knoll, A. H., Hurowitz, J., Baum, M., Ehlmann, B. L., Head, J. W., & Steakley, K. (2021). A coupled model of episodic warming, oxidation and geochemical transitions on early Mars. *Nature Geoscience*, 14(3), 127–132. <https://doi.org/10.1038/s41561-021-00701-8>
- Zaki, A. S. (2022). Prolonged record of hydroclimatic changes at Antoniadi crater, Mars. *Zenodo*. <https://doi.org/10.5281/zenodo.7129969>
- Zaki, A. S., Davis, J. M., Edgett, K. S., Giegengack, R., Roige, M., Conway, S., et al. (2022). Fluvial depositional systems of the African humid period: An analog for an early, wet Mars in the Eastern Sahara. *Journal of Geophysical Research: Planets*, 127(5), e2021JE007087. <https://doi.org/10.1029/2021je007087>
- Zaki, A. S., Pain, C. F., Edgett, K. S., & Castellort, S. (2021). Global inventory of fluvial ridges on Earth and lessons applicable to Mars. *Earth-Science Reviews*, 216, 103561. <https://doi.org/10.1016/j.earscirev.2021.103561>